Supporting Information Appendix Sansone et al

"Packaging and transfer of mitochondrial DNA via exosomes regulate escape from dormancy in hormonal therapy resistant breast cancer"

Materials and Methods

Patient Plasma Collection

Human peripheral plasma samples (5-10ml) were obtained in EDTA tubes from 1) control healthy subjects, 2) patients with early stage breast cancer (who had their tumor surgically removed) and were cancer free, 3) de novo metastatic disease who had not started therapy and 4) in those with progression of metastatic disease on anti-estrogen therapy at Memorial Sloan Kettering Cancer Center and all pathologically confirmed. All individuals provided informed consent for blood donation on approved institutional protocols (MSKCC IRB 12-137). Once blood was drawn, plasma was isolated within 4 hours. No samples were frozen.

Isolation and Nuclease treatment of EVs

Briefly plasma and conditioned media was centrifuged at 3000*g* for 20 min to remove any cell contamination. To remove apoptotic bodies, mitochondrial particles and large cell debris, the supernatants were centrifuged at 12,000*g* for 30 min. EVs were collected by spinning at 100,000*g* for 70 min. EVs were resuspended in 25ml of 1X PBS and loaded on a 5 ml 30% sucrose cushion (300g/L sucrose, 24g/L Tris base, pH 7.4). Samples were centrifuged at 100,000x*g* for 90' at 4°C. 3.5ml of the cushion, containing EVs, was diluted with 1X PBS and centrifuged at 100,000x*g* for 90' at 4°C. The EV containing pellet was resuspended in 25µl of PBS. Prior EV RNA/DNA isolation, EVs were treated with 1U of Baseline-ZERO™DNase0 (Epicentre), in order to eliminate contaminating ss- and ds-DNA, and processed with different nucleases to analyze its

chemical and physical status. Enzymes were heat inactivated with an incubation of 10 minutes at 70°C.

In vivo studies: EV education of hormonal therapy resistant experimental breast cancer

All cancer cell lines were engineered to express a GFP positive luciferase expression vector for in vitro and in vivo imaging studies. Prior to in vivo inoculation, cancer cells were FACS sorted (for GFP) and injected bilaterally in the mammary fat pads of 5-7 weeks old non-obese diabetic/severe combined immunodeficiency mice (NOD/SCID, obtained from NCI Frederick, MD). Pre-clinical therapeutic trials were generated using xenografts from tumorigenic MCF7 and ZR751 clones treated with tamoxifen pellet or fulvestrant (Faslodex, HT, AstraZeneca), which was given intra-muscularly in the posterior/popliteal muscles (100mg/injection/weekly). The in vivo role of $mtDNA_{+}$CAF-EVs in the promotion of HTR disease (Fig. 4*D* and Fig. 5*G*) was determined by first injecting HT-naïve cells (10^5 MCF7/ZR751) into the MFPs of NOD/SCID mice followed by the injection of $3x10^9$ CAF-EVs ($mtDNA^{hi}$-EV or $mtDNA^{lo}$-EVs; n=5 mice/group) into the venous circulation (retro-orbital injection, $3X10^9$ particles/mouse/weekly) of mice. EV number was determined by Nanosight analysis. After 8 weeks, once tumors were established (~1cm, BLI $2x10^9$), HT (fulvestrant, 100mg/mouse/weekly) was administered for an additional 6 weeks. For each in vivo experiment, cancer cells were mixed with an equal volume of Matrigel™ (BD Biosciences) in a total volume of 50µl. Bioluminescence (BLI: Xenogen, Ivis System) was used to monitor both tumor growth (weekly) and metastatic burden (at necropsy). For metastatic assays, primary tumors were removed from mice bearing MCF7 xenografts and metastatic progression was followed by BLI in

the presence of tamoxifen (pellet). All the surgical procedures and animal care followed the institutional guidelines and an approved protocol from our IACUC at MSKCC.

Cell lines and primary cultures

Human cancer cell lines (Hela, Caski -cervical carcinoma-), human breast cancer cell lines (MCF7, ZR751, T47D, and BT474), human bone marrow stromal cell lines (HS5, HS27a) and human normal fibroblasts (MRC5, HMF) were purchased from the American Type Culture Collection (ATCC). Murine CAFs (mCAFs) were isolated from xenografts by FACS purification (GFP negative, EpCAM negative). All cells were mycoplasma free and maintained in MEM and RPMI (ATCC and MSKCC Media Core) supplemented with 5% fetal bovine serum (Media Core), 2mM glutamine, 100units ml^{-1} penicillin, and 0.1mg ml^{-1} streptomycin (Media Core).

Analysis of Mitochondrial function

For in vitro labeling of mitochondria, MitoTracker dye was used (Invitrogen). For mitochondrial membrane potential TMRE was used according to manufacturer's protocol (Abcam, ab113852). Analysis of mitochondria function (fluorescence) was performed at the confocal microscopy (MSKCC). To measure mitochondrial complex activity, cell pellets were resuspended in assay buffer (125mM sucrose, 0.1mM EDTA, 25mM Tris-HCl pH 7.5, 0.025% Lauryl-β-D-maltoside), and enzymatic activities were assayed with $0.1–0.4 \cdot 10^6$ cells/ml at 25ºC spectrophotometrically. NADH:HAR reductase activity of Complex I was measured as a decrease in absorption at 340 nm (ε_{340nm} = 6.22 $mM^{-1}cm^1$) with 200μM NADH, 1mM HAR and 1mM KCN. Complex IV activity was measured as cytochrome oxidation at 550nm (ε_{550nm}= 21.5mM-cm-) with 50μM ferrocytochrome *c*. Activities are expressed in μmol of substrate$\cdot min^{-1} \cdot$mg of $protein^{-1}$. For protein measurement cells were pelleted and resuspended in 1% deoxycholate. Protein content was determined with a BCA assay.

Electron Microscopy (EM)

Cells were washed with serum-free media or appropriate buffer. Both EVs and cells were fixed with a modified Karmovsky's fix of 2.5% glutaraldehyde, 4% paraformaldehyde and 0.02% picric acid in 0.1M sodium caocdylate buffer at pH 7.2. Following a secondary fixation in 1% osmium tetroxide and 1.5% potassium ferricyanide, samples were dehydrated through a graded ethanol series and embedded in an epon analog resin. Ultrathin sections were cut using a Fiatome diamond knife (Diatome, USA, Hatfield, PA) on a Leica Ultracut S ultramicrotome (Leica, Vienna, Austria). Sections were collected on copper grids further contrastated with lead citrate and viewed on a JEM 1400 electron microscope (JEOL, USA, Inc., Peabody, MA) operated at 120 kV. Images were recorded with a Veleta 2K x2K digital camera (Olympus-SIS, Germany).

Nucleic acid extraction

DNA extraction: cell pellets and EVs (ultracentrifugation of 10^{12} cells) were resuspended in 25µl of 1X PBS followed by the addition of 450µl of DNA extraction buffer (SDS 0.5-1%, Tris-HCl 50mM pH 8.0, EDTA 0.1M) and 0,1mg/ml proteinase K 20mg/ml (ThermoFisher Scientific) and incubated O/N at 56°C. 500µl of phenol/chloroform (ThermoFisher Scientific) was added to each sample and centrifuged at 13,000 rpm for 5' at room temperature. The upper phase, containing the DNA, was transferred to a new tube where 500µl of chloroform were added. Samples were centrifuged at 13,000 rpm for 5' at room temperature; the DNA was washed a second time by repeating this step. The upper phase was transferred to a new tube with 450µl of isopropanol and 50µl of NaAc 3M. The samples were centrifuged at 13,000 rpm for 10' at 4°C. The supernatant was discarded and the pellet washed with 750µl 70% EtOH and centrifuged at 13,000 rpm for 5' at 4°C. The DNA pellet was air dried, resuspended in 20µl of DEPC H_2O and incubated at 37°C for 30'. DNA concentration was measured by loading 1µl of DNA on a Thermo Scientific NanoDrop™ 1000 Spectrophotometer and stored at -20°C until further

analyzed. For RNA extraction we used trizol (Invitrogen). EVs were suspended in 500µl of Trizol and vigorously mixed. The samples were centrifuged at 12,000x*g* for 30 seconds. 200µl of chloroform were added, mixed by inversion and incubated for 2-3' at RT. After a centrifugation at 12,000xg for 15' at 4°C, the upper phase was transferred to a new tube. 400µl of isopropanol and 3µl of glycogen were added to the sample and incubated O/N at -20°C; the samples were then centrifuged at 12,000xg for 10' at 4°C. The supernatant was discarded and the pellet washed in 750µl of cold 75% EtOH. The RNA was pelleted with a centrifugation at 8,000xg for 20' at 4°C, air dried and suspended in 10µl of DEPC H_2O. The RNA concentration was measured with a Thermo Scientific NanoDrop™ 1000 Spectrophotometer and treated for 1 hour at 37°C with 1U (for EVs) or 2U (for cells) of Baseline-ZERO™ DNase (Epicentre®). RNA was stored at -80°C.

Reverse Transcription PCR (RT-PCR) and microarray analyses

cDNA was obtained by retro transcribing 1µg of RNA -previously treated with 1U (EVs) or 2U (cells) of Baseline-ZERO™ DNase0 (Epicentre®)- and using iScript™Select cDNA synthesis Kit (Bio-Rad). The cDNA was kept at -80°C for further analysis. For microarray analysis 250ng of RNA was processed, assayed and run on Illumina GX Human HT12 platform prepared according to the manufacture's' protocol at the Genomic Molecular Core Facility (MSKCC). Data were analyzed, submitted at GEO (GSE84104).

Rolling Circle PCR and canonical PCR

DNA was isolated using phenol/chloroform (ThermoFisher Scientific). Each amplification reaction was performed on a total of 20ng of DNA using the GeneAmp® PCR System 9700, version 2.5. The amplification program was the following: (i) Polymerase activation (2 min at 95°C), (ii) amplification stage (35 cycles, with each cycle consisting of 30 seconds at 95°C, 30 seconds at 60°C, and 60 seconds at 72°C), and (iii) extension stage (5 min at 72°C). All amplification reactions were performed using the GoTaq®Flexi

DNA Polymerase kit (Promega). PCR products were resolved on a 2% agarose gel. All primers used for this assay are listed at the end of the methods section. Rolling Circle amplification (RCA) was performed in EV-DNA according to the manufacturer's protocol (GE Healthcare Life Sciences): 1) EV-DNA was first digested with Plasmid Safe ATP-DNAse (Epicentre®, 1U for 1 hour at 37°C) in order to degrade all non circular DNA 2) 10ng of previously digested EV-DNA was amplified using RCA methodology 3) 2ng of post-RCA amplicons were then amplified using qPCR with specific mtDNA and housekeeping DNA primers (Fig. S3*D* and Table S4).

Real time PCR

DNA and cDNAs were amplified by quantitative PCR (qPCR) using the Applied Biosystem Viia™ 7 Real-Time PCR System in the Power SYBR® Green PCR Master Mix Buffer. Each sample was run in triplicate. DNA amplification was performed on 2ng DNA/reaction; cDNA amplification was performed on 1μl of the cDNA/triplicate. All primers used in the Real Time assay are listed at the end of the section. For analysis, $\Delta\Delta_{ct}$ method was applied and fold change was calculated ($2^{-\Delta\Delta ct}$). In order to verify the specificity of the amplicons, other than the analysis of the Melting Temperature, amplicons were visualized on a 2% agarose gel using the ChemiDoc™ XRS+ System (Bio-Rad).

EV labeling and transfer to recipient cells

EVs from CAFs, were labeled using the PKH67 Green Fluorescent Cell Linker Kit for General Cell Membrane Labeling (Sigma-Aldrich) and Ethidium bromide (EtBr, 1.5ng/sample) for DNA staining. 10^5 HTD cells (MCF7 cells treated with HT-see description of cell lines) were grown in Nunc®Lab-Tek®Chamber Slide (Sigma-Aldrich), had been previously coated with fibronectin to allow for cell adhesion. Cells were then treated with 3X{10^{7-8}} labeled EVs and their localization determined 48 hours later.

Mitochondria were labeled using Red-MitoTracker® (25nM for 30 minutes at 37°C). Cells were washed and fixed (4% paraformaldehyde) and nuclei were stained with DAPI. Fluorescent confocal microscopy (Nikon Eclipse TE2000U) was used to localize EVs (green channel-PKH67), mitochondria (red channel) and nuclei acid (far red for EtBr) and analyzed using Nikon software (EZ-C1 3.6).

Protein, Immunohistochemistry and in vitro studies

For immunoblotting assays, cells were lysed in buffer (50mmol/L Tris at pH 7.5, 150mmol/L NaCl, 5μg/mL aprotinin, pepstatin, 1% NP-40, 1mmol/L EDTA, 0.25% deoxycholate, and protease inhibitor cocktail tablet, Sigma). Proteins were separated by SDS-PAGE, transferred to PVDF membranes, and blotted with specific antibodies: OXPHOS complex Antibody (Invitrogen, 45-7999, this antibody recognizes the mitochondrial subunit ATP5A1); tubulin (Santa Cruz Biotech. Inc: 10D8); Cd63 (EXOAB-CD63A-1, System Bioscience) and Actin (Santa Cruz Biotech. Inc). For immunostaining assays: organs were collected and fixed overnight in 4% paraformaldehyde, washed, embedded in paraffin and sectioned (Histo-Serve). H&E staining was performed by standard methods. The enrichment of CAFs in xenografts was determined by desmin immunohistochemistry (IHC) in tumour-derived sections. IHC was performed on Leica Bond RX (Leica Biosystems) with 1μg/ml Desmin Rabbit polyclonal antibody (Abcam cat#ab8592). For determination of cell viability, we seeded 2,500 cells per well in 96-well plates and treated them with fulvestrant (10μM). Viable cells were determined 7-14 days after treatment using trypan blue and cell counting using bright field microscopy or DAPI exclusion staining by flow cytometry (Dako Cytomation). Proliferation assays were carried out using CalceinAM technology (Invitrogen) or bioluminescence: cells were seeded in 96 wells plates treated with the pre-fluorescent/luciferin compound for 20min

and fluorescence/bioluminescence was read using a plate reader (SpectraMax plate platform/IVIS BLI xenogen).

Semi-Quantitative Mass Spectrometry analysis of CAF EV

Mass spectrometry analyses of EV were performed at the Rockefeller University Proteomics Resource Center (New York, NY, USA) using 10μg of CAF-EV protein. Samples were denatured using 8M urea, reduced using 10mM dithiothreitol, and alkylated using 100mM iodoacetamide, followed by proteolytic digestion with endoproteinase LysC (Wako Chemicals), and subsequent digestion with trypsin (Promega) for 5 hours at 37 °C and quenched with formic acid and the resulting peptide mixtures were desalted. Samples were dried and solubilized in buffer containing 2% acetonitrile and 2% formic acid. Approximately 3–5 μg of each sample was analysed by reverse-phase nano-LC-MS/MS (Ultimate 3000 coupled to QExactive, Thermo Scientific). Following loading on the C18 trap column (5 μm beads, Thermo Scientific) at a flow rate of 3μl min^{-1}, peptides were separated using a 75-μm-inner-diameter C18 column (3 μm beads Nikkyo Technos) at a flow rate of 200nl min^{-1}, with a gradient increasing from 5% Buffer B (0.1% formic acid in acetonitrile)/95% Buffer A (0.1% formic acid) to 40% Buffer B/60% Buffer A, over 140 minutes. All LC-MS/MS experiments were performed in data-dependent mode. Precursor mass spectra were recorded in a 300–1,400 *m*/*z* mass range at 70,000 resolution, and 17,500 resolution for fragment ions (lowest mass: *m*/*z* 100). Data were recorded in profile mode. Up to 20 precursors per cycle were selected for fragmentation and dynamic exclusion was set to 45 seconds. Normalized collision energy was set to 27. Data were extracted and searched against Uniprot complete Mouse proteome databases (January 2013) concatenated with common contaminants using Proteome Discoverer 1.4 (Thermo Scientific) and Mascot 2.4 (Matrix Science). All cysteine residues were considered alkylated with acetamide. Amino-terminal glutamate to pyroglutamate conversion, oxidation of methionine, and

protein N-terminal acetylation were allowed as variable modifications. Data were first searched using fully tryptic constraints. Matched peptides were filtered using a Percolator-based 1% false discovery rate. Spectra not being matched at a false discovery rate of 1% or better were re-searched allowing for semi-tryptic peptides. The average area of the three most abundant peptides for a matched protein was used to gauge protein amounts within and in between samples.

FACS Analysis

Human cancer cell lines (MCF7, ZR751, T47D, and BT474), were engineered to express a GFP/Luciferase vector. Cancer cells from xenografts were isolated from primary and metastatic tissues by enzymatic digestion (Collagenase/Hyaluronidase, Sigma-Aldrich), sorted ($GFP^+/DAPI^-$) and cultured in vitro. For FACS/Flow analyses xenograft derived tumors and metastases were digested in sterile Epicult media (Stem Cell Technology), minced with sterile razor blades and incubated for 3 hours in the presence of Collagenase/Hyaluronidase (1,000Units/sample, Voden Medical). Cells were washed with PBS supplemented with 1% bovine serum albumin (PBS-BSA 1%) and filtered through a 40μM nylon mesh (BD Biosciences). For the detection of CD44 and CD133, EpCAM antigens, cells were stained in a volume of 100μl (PBS-BSA 1%) with each antibody CD44-APC (100ng/10^6 -10^8 cells Clone IM7, eBiosciences), CD133/1-PE (100ng/10^6 to-10^8 cells, clone AC133, Miltenyl Biotech) and EpCAM-FITC (250ng/10^6 to-10^8 cells, Clone VU-1D9, Stem Cell Technologies). Cells were labeled on ice for 30 min and analyzed (BD FACS Aria III, Flow Core). Samples were analyzed for cell population distribution and sorted for GFP/viability ($GFP^+/DAPI^-$) and CD133/CD44 expression. For flow plot analyses, samples were run using FlowJo 7.5 software (Tree Star).

Primers

The reference sequences used for primers design are NC_010339 for the murine mitochondrial DNA/RNA, NC_012920 for the Human mitochondrial DNA/RNA (*SI Appendix*, Table S4).

Exit from dormancy via CAF-EVs

Generation of HTD cells was performed by treating ER+ (GFP+) breast cancer cell lines (MCF7, ZR751, BT474) with HT (fulvestrant, 10μM) for 2 months. Single, non-proliferating cancer cells were FACS purified by gating on GFP+ cells and by DAPI exclusion staining by flow cytometry (Dako Cytomation). Viable cell number was subsequently determined using trypan blue exclusion and cell counting using bright field microscopy HTD cells were then cultured in vitro or injected in vivo for further studies. In vitro assays: HTD cell were cultured in 96-well dishes (1000 cells/well) and treated with 10^7 EVs (mtDNA^{hi}-EV or mtDNA^{lo}-EVs) weekly (4x). Half of the cultures were also treated with HT (fulvestrant, 10μM, Sigma-Aldrich). Proliferation was determined by Calcein AM assay (InVitrogen). HTD were cultured in low attachment (Corning) 24-well plates. These were treated with $3x10^9$ mCAF-derived EVs (wt-mtDNA^{hi} or ρ0-mtDNA^{lo}) weekly x4 in the presence with HT (fulvestrant, 10μM/weekly). After 40 days, mammosphere number (bright field microscopy) was determined after 40 days. In vivo assays: Dormant ZR751 cells (HTD) were isolated and 10^5 cells were injected in the IV inguinal MFP of NOD/SCID mice. All mice were subsequently injected with $3x10^9$ mCAF-derived EVs (wt-mtDNA^{hi} or ρ0-mtDNA^{lo}) weekly x8 (n=5 mice/group). Tumor growth was determined by BLI and after necropsy.

Immunogold Electron microscopy: exogenous EVs fusing with mitochondria

Breast cancer cells (MDA-MB 231) were educated with B16F10 (murine melanoma cell line) EVs for 48 hours; cells were fixed with 2%PFA in 0.1M sodium cacodylate, pH 7.4

for 24 hours at 4 C. Cells were blocked using 3%BSA, 0.1% saponin in 0.1M sodium cacodylate and incubated overnight with a murine TSG101antibody (Novus NBP1-80244) diluted to 1:300 in blocking solution. After washing in 0.1% saponin and 0.1M sodium cacodylate, cells were incubated with secondary antibody (Biotin anti-Rabbit, Vector Labs Cat#BA-2000) diluted to 1:1000 in blocking solution for 2 hours and washed again. Finally, cells were incubated with Alexa Fluor488 streptavidin FluoroNanogold (Nanoprobes, Cat#7216) diluted to 1:50 in blocking solution for 2 hours, washed and fixed in 2.5% glutaraldehyde overnight at 4^0C. HQ Silver enhancement (Nanoprobes, Cat#2012) was performed for three minutes. TSG101 localization was confirmed using immunofluorescence before electron microscopy processing.

Electron Microscopy Processing

Sections were post-fixed in 1% Osmium tetroxide in 0.1M sodium cacodylate for 60 minutes on ice. After washing with water, cells were placed in 1% aqueous uranyl acetate for 30 minutes, dehydrated in a graded series of ethanol and embedded in Eponate. Sections were cut at 70nm, transferred to formvar coated slot grids and imaged on a JEOL 100CX at 80kVwith an AMT XR41 digital imaging system (Rockefeller University Electron Microscopy Core Center).

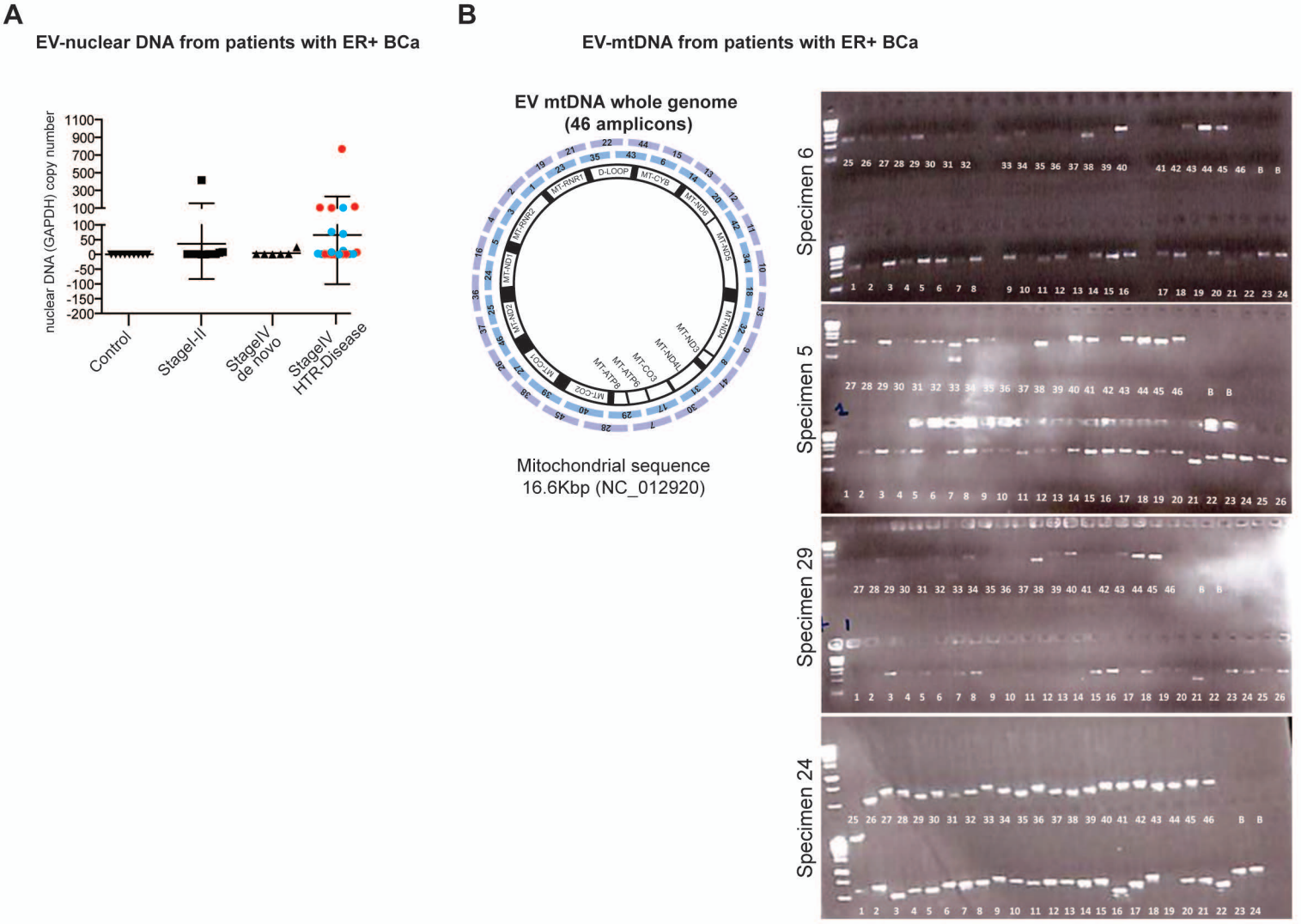

Fig. S1. Circulating EV DNA is enriched for whole mtDNA genome. (*A*) Dot plot of nuclear DNA copy number quantification as determined by qPCR for *GAPDH* gene in circulating EVs isolated from fresh collected plasma (5-8ml) of 8 healthy controls and 20 luminal breast cancer patients at different stage of their disease (*SI Appendix*, Table S1). Each point corresponds to a pateint sample. (*B*) Schematic and gel electrophoresis of whole mtDNA genome amplified in several patient derived circulating EV-DNA resulting from 46 overlapping PCR amplicons to cover all the mtDNA genome.

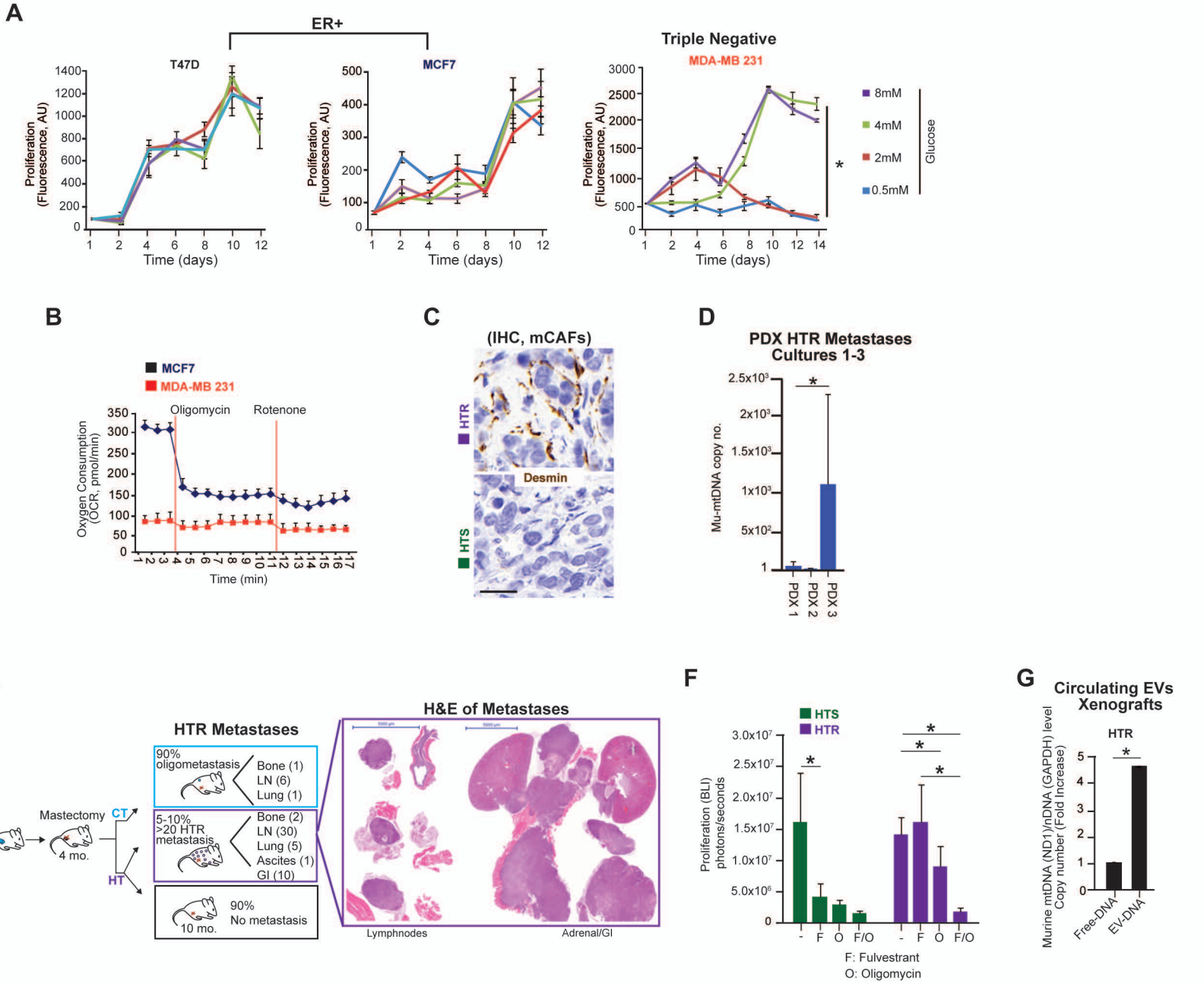

Fig. S2. OXPHOS inhibition abrogates HTR disease. (*A*) Proliferation potential as determined by in vitro cell growth (CalceinAM, fluorescence) in luminal (ER+) and triple negative cancer cell lines cultured in media with increasing concentration of glucose. (*B*) Oxygen consumption rates (OCR) ±oligomycin (200nM)/rotenone (100nM) in MCF7 and MDA-MB-231 cells as determined by seahorse technology.(*C*) Desmin immunohistochemical images of mCAFs in HTS/HTR-derived tissues (scale bar 25μm). (*D*) Murine (Mu)-mtDNA level as copy number (qPCR, *ND1*) in FACS (Epcam+/Dapi-) purified cancer cells from 3 different PDX cultures (PDX 1-3) generated from patient bone breast cancer metastases injected in the mammary fat pad of nude mice (see *SI Appendix, Materials and Methods*). (*E*) Schematic analysis of the generation of metastatic HTR disease in mice. Following 4 months from primary tumor xenografts (MCF7), tumor tissues were removed and mice were randomized to recieve HT (fulvestrant, 100μg/injection/weekly). Metastatic burden was analyzed by BLI and at necropsy by histological examination (H&E). (*F*) Proliferation potential in presence of oligomycin (100nM) and ±HT as determined by in vitro BLI in metastatic cells from HTS and HTR cells FACS purified from xenografts (Fig.2*A*). Error bars, mean±s.d. of BLI from n=3 samples. (*G*) mtDNA/nDNA level in circulating EVs from HTR xenografts as determined by copy number (*GAPDH, ND1*: qPCR Fold change). Data are reported as error bars, mean±s.d. of n=3 independent experiments (*A*, *D-G*). **P*<0.05 (Student's t-test) and GLM anova after multiple comparisons (*A*).

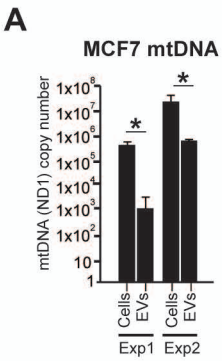

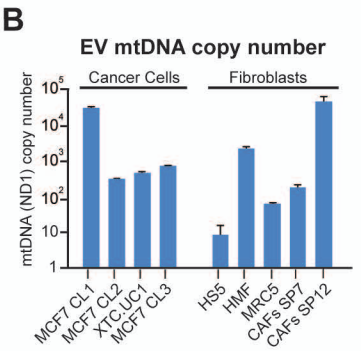

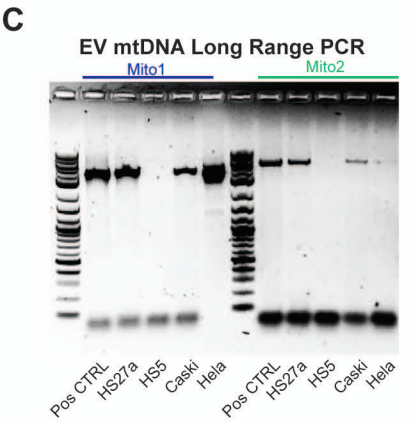

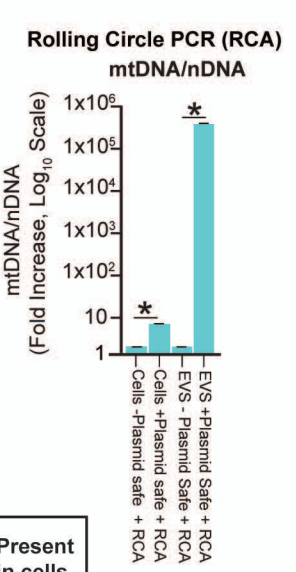

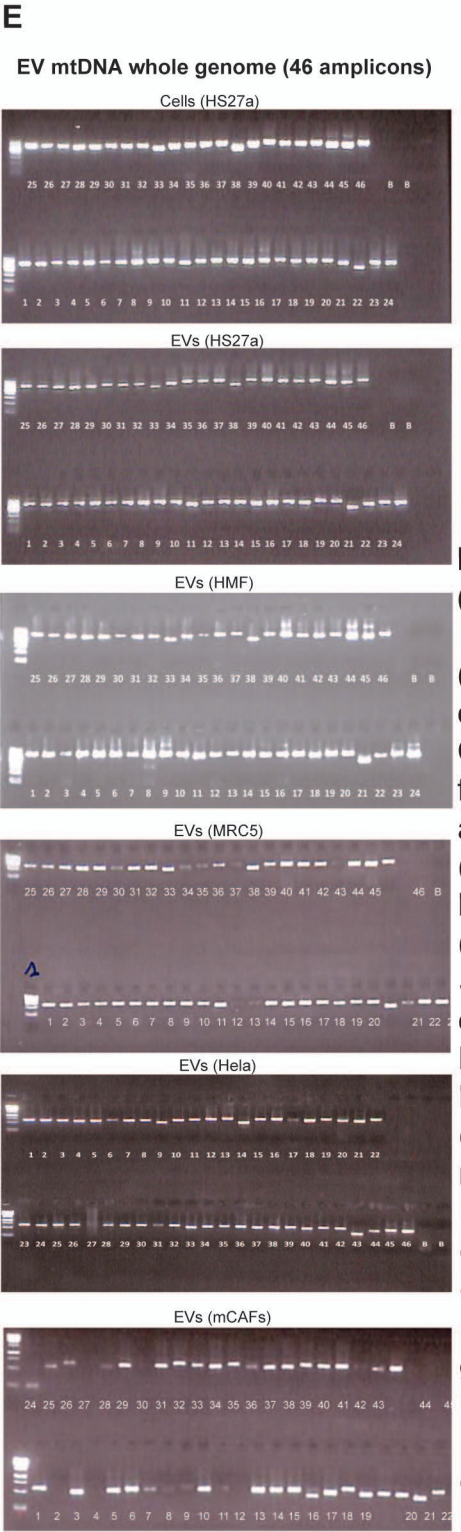

F

Genetic characterization of EV mtDNA

Cell line	Genetic variants mtDNA position	Gene	Present in cells
HS27a EVs	m.571C>A	D-LOOP	YES
	m.1102A>G	MT-RNR1	YES
	m.3550G>R	MT-ND1	YES
	m.3741C>T	MT-ND1	YES
	m.5529A>G	MT-TW	YES
	m.8684C>T	MT-ATP6	YES
HMF EVs	m.9150A>G	MT-ATP6	YES
	m.9380G>A	MT-CO3	YES

Fig. S3. The entire mtDNA genome is present in EVs.
(*A*) Bar graph showing human mtDNA copy number (*ND1*) in MCF7 cells and EVs from two different experiments.
(*B*) Bar graph of human mtDNA copy number in EV (10^{13}) isolated from the conditioned media of human cancer cells and fibroblasts ($5*10^7$ cells). CL1-3, xenograft derived MCF7 derivatives; HMF, normal mammary gland fibroblasts; MRC5,normal lung fibroblasts; CAFs SP, patient derived cancer associated fibroblast cultures; HS5, human bone marrow stromal cell line.
(*C*) Representative gel electrophoresis images of mtDNA PCR amplicons Mito1/2 derived from EV-DNA. Pos CTRL, cellular derived DNA (HS27a).
(*D*) EV-DNA 1) was isolated from 10^{13} mCAF-derived EVs (see *SI Appendix, Materials and Methods*) EV were pretreated with DNAse0 to devoid of cell free DNA contamination), 2) EV-DNA was digested with Plasmid Safe DNAse (1u/sample) to degrade non circular DNA, 3) 10ng of digested and ctrl EV-DNA (- Plasmid safe DNAse) was amplified using rolling circle PCR assay (RCA), 4) 2ng of post RCA product was then amplified using specific mtDNA or nDNA primers by qPCR (Mu-*ND1* and Mu-*GAPDH*, *SI Appendix*, Table S4). Ratio of mtDNA/nDNA level by qPCR is shown as error bars, mean±s.d. (Fold Increase).
(*E*) Gel electrophoresis of whole mtDNA genome amplified in EV-DNA resulting from 46 overlapping PCR amplicons to cover all the mtDNA genome from multiple fibroblast and cancer cell lines.
(*F*) Table representing mtDNA mutations and SNPs in EVs and cells from HS27a and HMF cell lines.Data are reported as error bars, mean±s.d. of n=3 independent experiments (*A*, *D*); **P*<0.05 (Student's t-test).

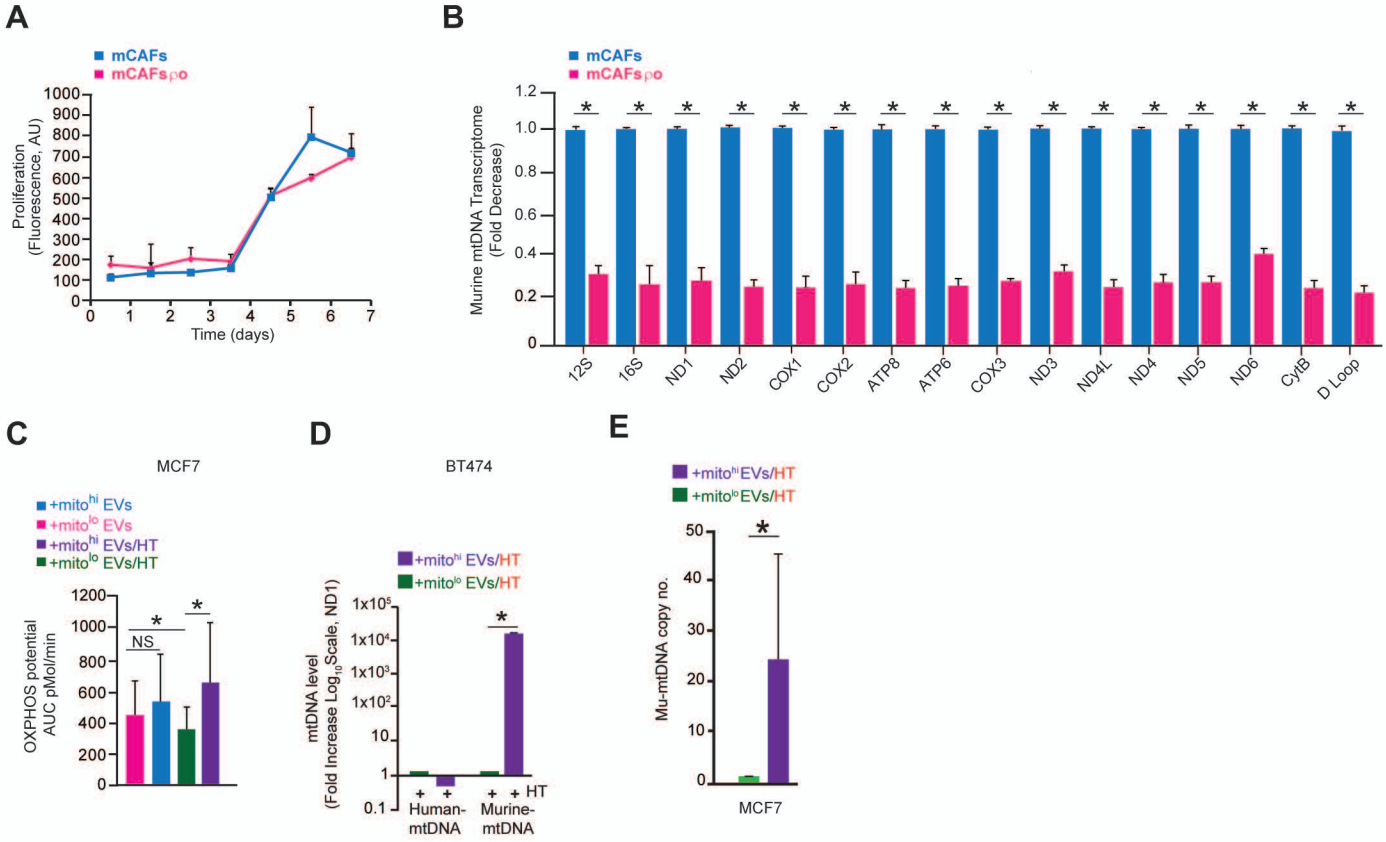

Fig. S4. Depletion of mitochondria DNA in CAFs hampered the EV-dependent up-regulation of OXPHOS potential in HT cells.

(*A*) Proliferation potential as determined by in vitro cell growth (CalceinAM) in mCAFs (wild type or ρ0). (*B*) Mitochondrial transcriptome as determined by qPCR in mCAFs cells (wild type or ρ0). Error bars, mean±s.d of fold change (reference wild type).*P<0.05 (Student's t-test). (*C*) OXPHOS potential in cancer cells ±HT (fulvestrant, 10μM) administered for 48 hours with mito^{lo}-EVs and mito^{hi} EVs (10^{13}EVs for 10^6 cells). Error bars, mean±s.d of respiration rate under mitochondrial stressors (FCCP, oligomycin, rotenone).*P<0.05 (Student's t-test). (*D*) mtDNA level (qPCR, *ND1*) in HTS and HTR cells ±HT from Fig.4*C* (fulvestrant, 10μM). Error bars, mean±s.d. of fold change (reference HTS). (*E*) Murine (Mu)-mtDNA level as copy number (qPCR, *ND1*) in FACS (GFP+/Dapi-) purified cancer cells from xenografts (Fig.4*D*).*P<0.05 (Student's t-test).

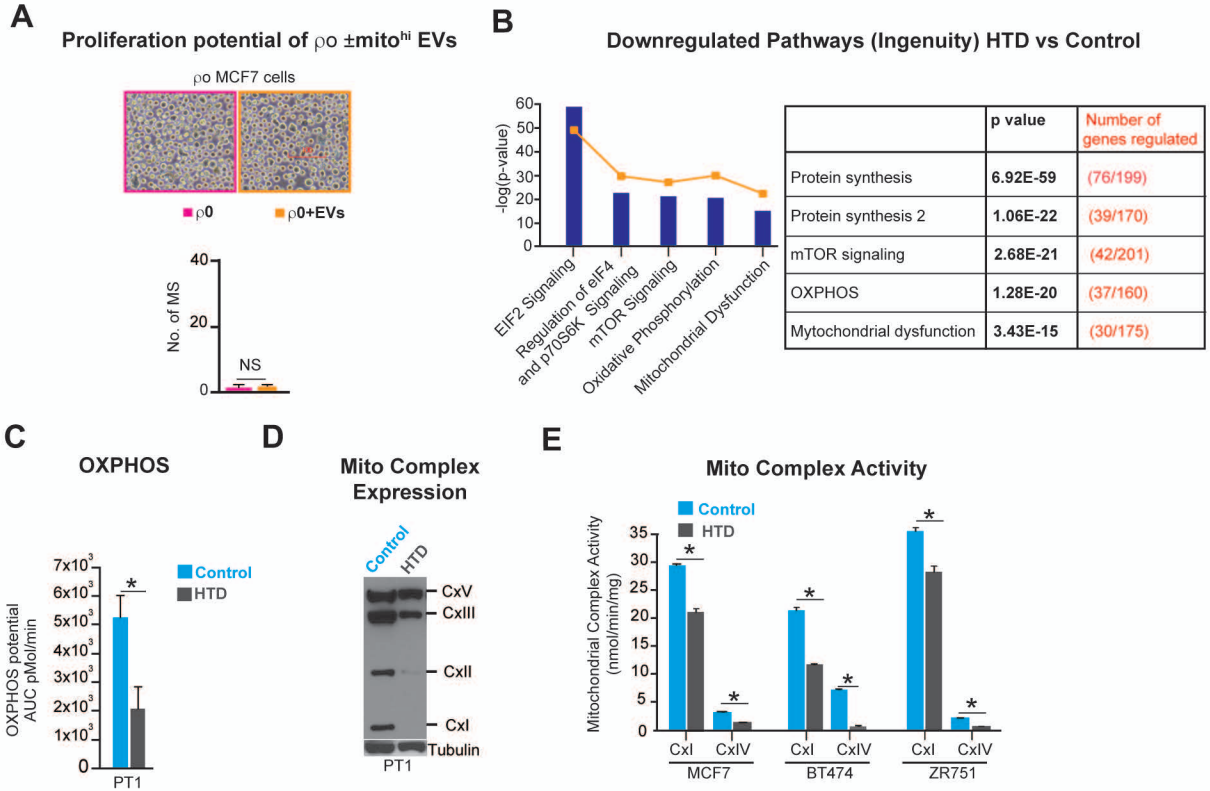

Fig. S5. HT induced metabolic dormancy and reduction of mtDNA level.
(*A*) Representative bright field images of MCF7 ρo cells ± mito^{hi} CAF-EVs (3*10^9/weekly for 40 days). Bar graph of number of MS is also reported at the endpoint of the experiment (40 days). (*B*) HT led to decreased expression of mRNA involved in protein synthesis and OXPHOS signaling with z score and -log (p-values)- as determined by Ingenuity analysis of microarray data from RNA isolated Fig.5*A* (MCF7), single P values are also reported.
(*C*) OXPHOS potential determined as changes of respiration rate under mitochondrial stressors by seahorse technology (oligomycin 1μM, rotenone 100nM) in cancer cells isolated from Fig.5*B* (MCF7, PT1).
(*D*) Western Blot analysis of OXPHOS protein cocktail in cells from panel *C*. (*D*) Mitochondrial Complex I/IV activity quantification as determined by nmol/min/mg of protein in luminal breast cancer cell lines from panel *A*.
Data are reported as error bars, mean±s.d. of n=3 independent experiments (*C*, *E*); *P<0.05 (Student's t-test).

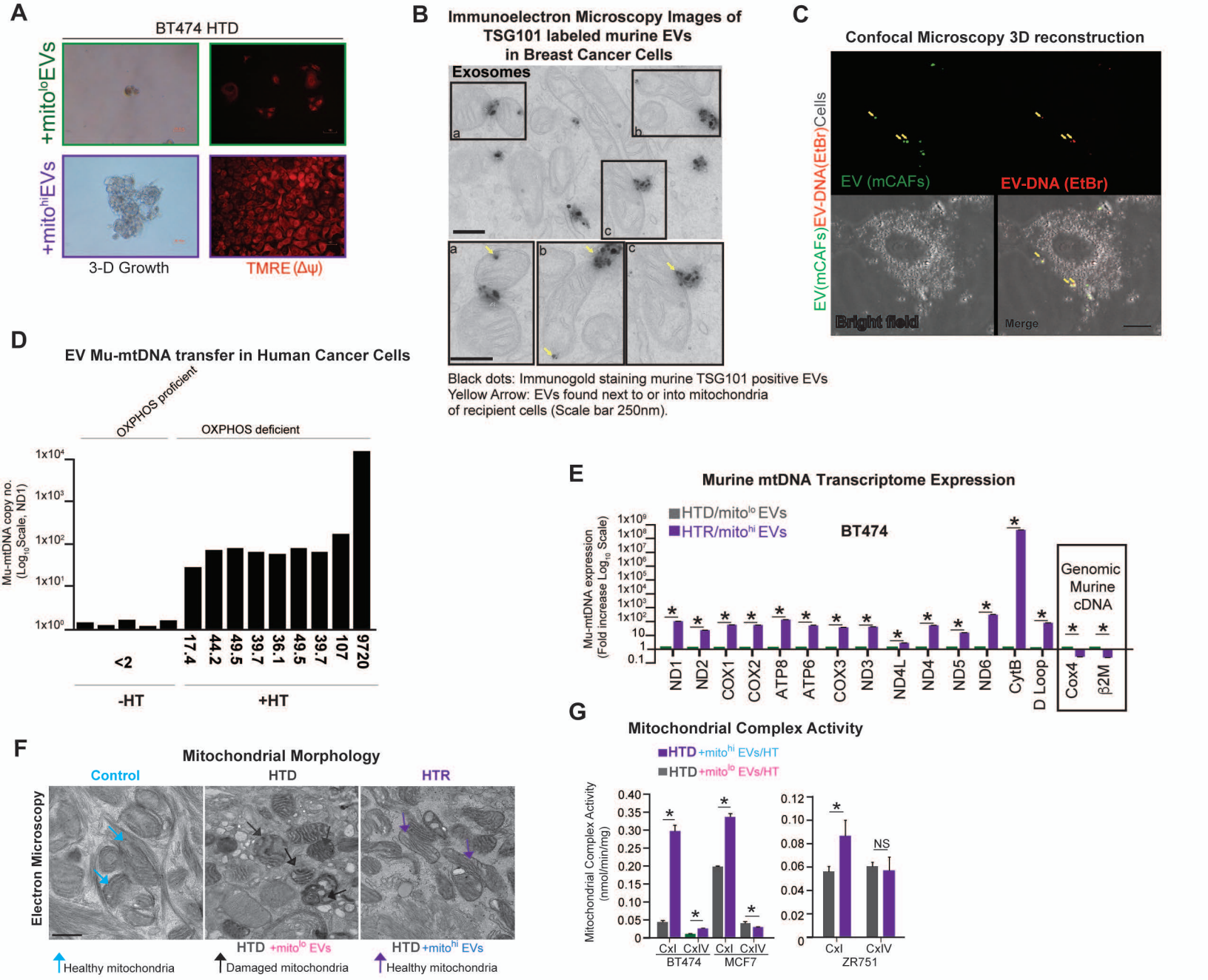

Fig. S6. Mito^{hi} EV educated HTR cells display proficient mitochondria. (*A*) Dormant MCF7/BT474 cells (HTD) were isolated (Fig. S5) and treated with 3*10^9 mCAF-derived EVs (wt-mtDNA^{hi} or ρ0-mtDNA^{lo}) weekly x4.After 40 days, 3D growth as mammosphere (and mitochondrial membrane potential (Δψ) by TMRE staining (red) were determined scale bar 100μm.(B) Representative TEM images of a recipient cell cytoplasm (mitochondria rich area, breast cancer cells) following exogenous labeled TSG101 exosome education (murine EV). Immunogold for murine TSG101 was performed (murine TSG101 antibody does not recognize human antigen). Scale bar 250nm (*C*) Confocal Microscopy images of HTD cells (MCF7) following labeled CAF-EVs administration: CAF-EVs were isolated from 3*10^9 mCAFs, labeled with PHK26 green (according to manufacturer's protocol) and EtBr (1.5 ng); PHK26^{pos}/EtBr^{pos} EVs were administered to cancer cells and 24h later confocal imaging was performed. Yellow arrows show colocalization of DNA and EVs. Scale bar 5μm. (*D*) Mu-mtDNA copy number (qPCR, *ND1*) from HTD MCF7 cells (different clones) and controls cultured in vitro and in vivo (MFP) with mCAF-EVs (3*10^9/weekly/1 month). (*E*) Murine mitochondrial RNA expression (as fold change -log10scale-) by qRT-PCR in HTR and HTS cells (reference HTDorm cells; BT474, see Fig. 5*E*); the expression of nuclear encoded murine (non-mitochondrial RNA) transcripts was also determined (Cox4, β2M). (*F*) Mitochondria morphology as determined by electron microscopy in the MCF7 model: cancer cells in absence of HT (control) and following HT-induced dormancy (HTD) ± CAF-EVs (mito^{lo} or mito^{hi}). Arrows shows damaged (loss of cristae, matrix-dense round mitochondria) and healthy mitochondria (↑). Scale bar 200nm. (*G*) Mitochondrial Complex I/IV activity quantification as determined by nmol/min/mg of protein in luminal breast cancer cell lines from panel a. Data are reported as error bars, mean±s.d. of n=3 independent experiments, *P<0.05 (Student's t-test).

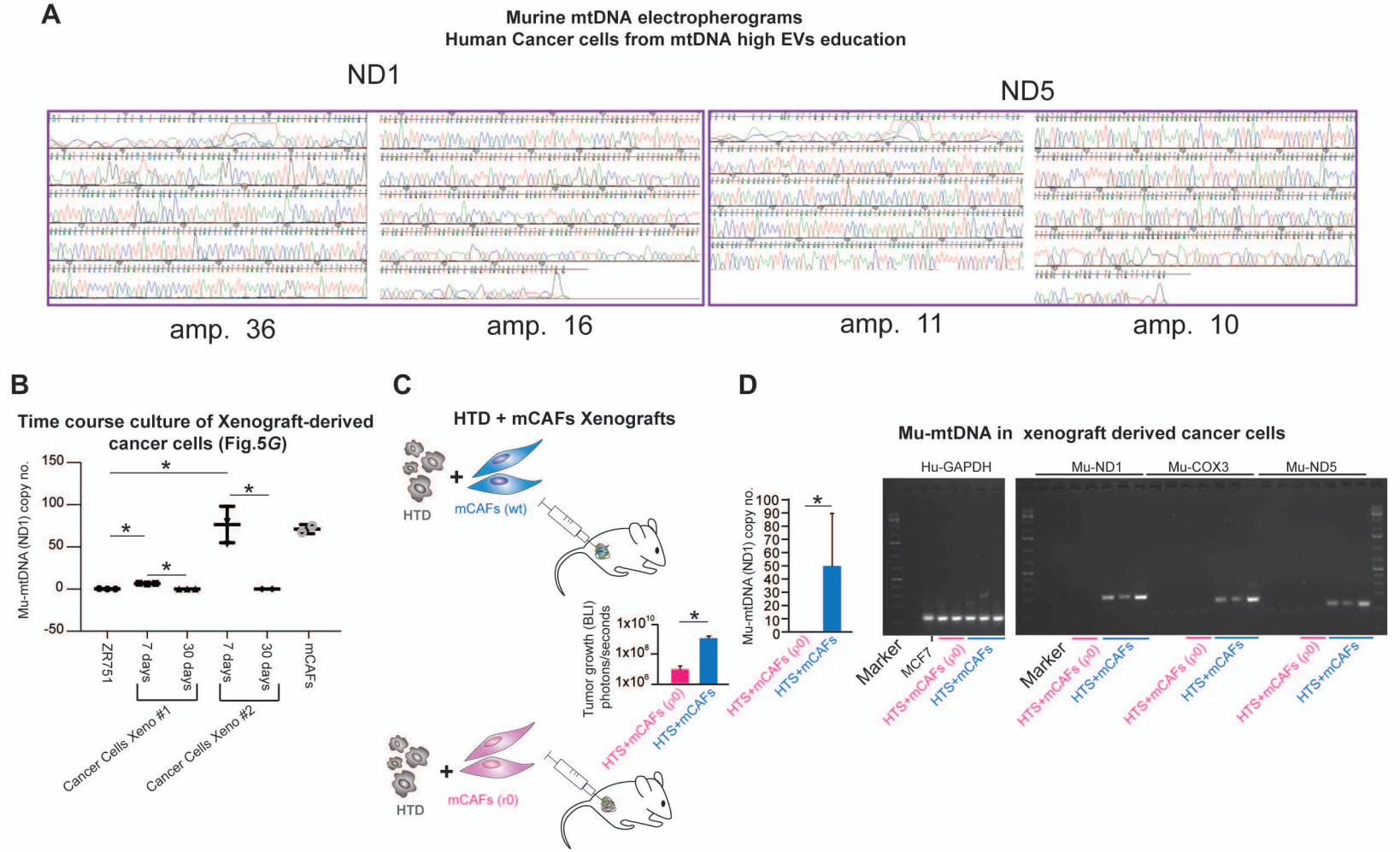

Fig. S7. Depletion of mtDNA abrogates the CAF-dependent tumorigenic potential of HTS cells.
(*A*) Representative electropherograms of *ND1* and *ND5* sequences (amplicons 36, 16, 11, 10) derived from whole murine mtDNA sequencing using a set of NumtS (nuclear mitochondrial sequences)-excluding overlapping primers in cancer cells from Figure 5*H* (see *SI Appendix, Materials and Methods*).(*B*) Dot plot of murine mtDNA level (*ND1* copy number) from FACS purified cancer cells derived from xenografts tissues of EV-treated mice and cultured in vitro for 30 days (2 different examples Xeno#1 and Xeno#2 and control are reported). Data are reported as error bars, mean±s.d. of n=3 samples. (*C*) Schematic of the experimental design: HTS cells (MCF7, Luciferase^{pos}) were originated *in vitro* following chronic fulvestrant administration (fulvestrant, 10μM/weekly for 2 months), were injected (10^5) into the MFP of mice in presence/absence of mCAFs (wild type or ρ0: 1:10=CAFs:MCF7). Tumor growth as BLI mean±s.d. was determined at the endpoint of the experiment (5 months from the injection, n=10 mice/group). *P<0.05 (Student's t-test).
(*D*) Murine mtDNA expression as mean±s.d. copy number (ND1, qPCR) in xenograft derived cancer cells FACS (GFP+) isolated at the endpoint of experiment panel *C*. Representative gel electrophoresis images of murine mtDNA sequences (*ND1, COX3, ND5*) expressed in tumor cells (distinct lesions) purified via FACS from xenografts (panel *C*). Data are reported as error bars, mean±s.d. of n=3 samples. *P<0.05 (Student's t-test).

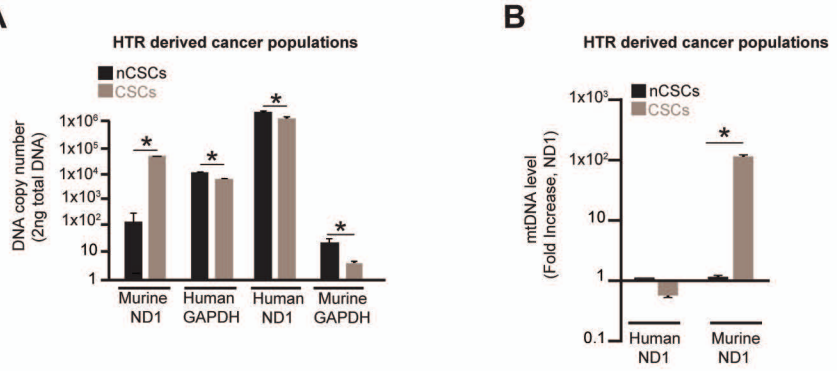

Fig. S8. The horizontal transfer of mtDNA occurs in cancer stem cell like cells in vivo.
(*A*) DNA copy number of murine and human mtDNA (*ND1*) and nDNA (*GAPDH*) in nCSCs ($CD44^{lo}CD133^{lo}$) and CSCs ($CD44^{hi}CD133^{hi}$) derived from HTR MCF7 cells *in vivo*. (*B*) mtDNA level (qPCR Fold Increase *ND1*, as reference nCSCs-*ND1* level) in nCSCs and CSCs cells from panel *A*. Data are reported as error bars, mean±s.d. of n=3 samples. *P<0.05 (Student's t-test).

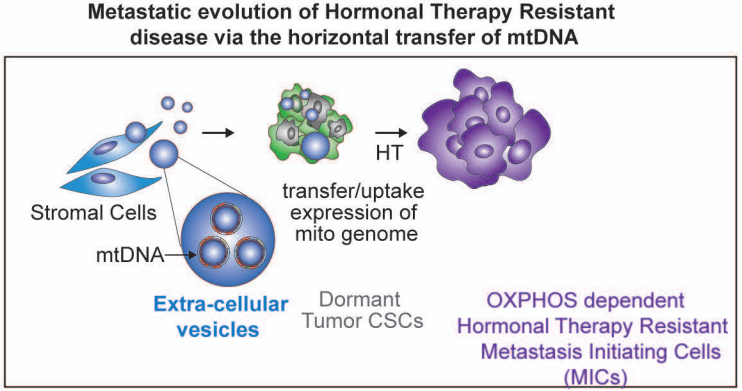

Fig. S9. EV-mediated horizontal transfer of mtDNA promotes HTR disease and exit from therapy-induced dormancy. The horizontal transfer of mtDNA promotes hormonal therapy resistance. Extracellular vesicles (EVs) from cancer-associated fibroblasts (CAFs) contain the whole mtDNA genome, which is transferred to HT-derived dormant CSCs promoting mitochondrial activity (OXPHOS) and HTR disease via increased OXPHOS dependent self-renewal of CSCs (metastasis initiating cells, MICs).

Table S1

	Patient #	Subtype	Disease Sites	Disease Volume	ND1 C# Mean	ND1 C# STD	GAPDH C# Mean	GAPDH C# STD
HTR Metastatic	21	IDC ER70 PR0	bone	high	ND	ND	1.08	0.50
	2	ILC ER100 PR50	pleura, skin	low	3505.61	893.91	12.58	2.49
	24	IDC ER90 PR5	Liver,bone, LN brain,	high	3006.89	188.26	ND	ND
	4	ILC ER50 PR0	LN, gastric	low	2037.19	195.66	69.79	3.76
	5	IDC ER60 PR0	bone, lymph node LN	high	1819.69	194.33	102.59	24.89
	51	IDC ER80 PR0	brain, bone, skin, LN	high	1167.87	31.23	7.23	2.25
	10	IDC ER80 PR10	liver, bone	high	990.82	57.42	117.19	14.26
	35	IDC ER100 PR50	plera, bone	low	837.71	188.90	1.65	0.52
	41	ILC ER80 PR0	orbit, bone,LN	high	834.69	177.56	1.45	0.44
	20	IDC ER95 PR60	lung	high	714.48	138.97	0.18	0.04
	9	IDC ER30 PR0	scalp, liver, bone, LN	high	694.30	29.51	105.67	12.93
	8	IDC ER80 PR10	LN, bone, breast	high	519.77	23.36	767.91	116.76
	7	IDC ER20 PR0	bone	low	417.38	6.45	103.77	15.24
	36	IDC ER50 PR0	skin, liver	low	390.35	15.74	7.74	1.68
	22	IDC ER50 PR0	Bone, LN	low	300.99	5.77	ND	ND
	15	IDC ER90 PR80	Bone	low	247.82	20.34	76.81	6.78
	18	IDC ER15 PR0	liver, pleura, skin, bone, LN	high	169.71	38.37	0.09	0.03
	19	IDC ER80 PR50	bone, lymph node LN	low	85.30	17.75	0.26	0.04
	17	IDC ER60 PR5	pleura, bone, liver	high	78.38	4.52	1.02	0.33
	46	ILC ER30 PR0	skin, peritoneum, LN	low	74.91	16.92	2.96	.15
	47	IDC ER80 PR50	lung, lymph node	low	10.90	3.39	1.00	0.82
	39	ILC ER60 PR10	orbit, pleura, bone, gastric	high	3.08	0.98	ND	ND

	Patient #	Subtype	Disease Sites	Disease Volume	ND1 C# Mean	ND1 C# STD	GAPDH C# Mean	GAPDH C# STD
De Novo Metastatc	30	IDC ER10 PR0	skin	low	ND	ND	ND	ND
	32	IDC ER80 PR50	bone, breast	high	6.22	0.24	24.04	11.23
	38	IDC ER100 PR10	breast, bone, LN	high	9.97	2.30	ND	ND
	40	ILC ER70PR0	breast, liver, LN	high	17.05	1.46	0.88	0.86
	37	IDC ER95 PR0	LN, gastric, bone, breast	low	42.29	13.62	0.68	0.24
	34	ILC ER80 PR80	breast, peritoneum, bone	low	ND	ND	0.06	0.06

	Patient #	Subtype	ND1 C# Mean	ND1 C# STD	GAPDH C# Mean	GAPDH C# STD
Stage 1-2	6	IDC ER70 PR20	7.08	4.23	1.10	0.78
	13	IDC ER100 PR50	1.58	1.71	6.02	9.42
	16	IDC ER20 PR0	ND	ND	ND	ND
	23	IDC ER90 PR90	6.31	2.69	ND	ND
	25	IDC ER100 PR90	ND	ND	ND	ND
	28	IDC ER50 PR20	ND	ND	ND	ND
	29	IDC ER80 PR0	42.08	7.51	8.09	2.23
	31	IDC ER100 PR70	ND	ND	ND	ND
	41	IDC ER90 PR80	2.83	0.47	415.96	169.74
	42	IDC ER30 PR0	8.93	3.53	ND	ND
	49	IDC ER60 PR10	2.77	2.35	0.35	0.19
	52	IDC ER90 PR60	ND	ND	0.20	0.04

Table S1. EV analysis from patients with HT-resistant (HTR) ER+/HER2- metastatic breast cancer and early stage disease 1. Subtype of Tumor: Invasive Lobular Carcinoma (ILC) or Invasive Ductal Carcinoma (IDC). Estrogen Receptor (ER) and Progesterone Receptor (PR) % Expression. 2. Disease Sites: Organs with metastatic disease. 3. Disease Volume: Low indicates <1% organ involvement; Hi indicates >10% organ involvement. 4. ND1 copy number/10ng of DNA and STD. 5. GAPDH copy number/10ng DNA and STD.

Table S2

	Cell Line	mtDNA position	Present in Evs	Gene	Predicted Functional
Significance: Mutations	HTS	m.3287C>A	Yes	MT-TL1	associated with encephalomyopathy
	HTS	m.9808C>T	Yes	MT-CO3	novel, predicted damaging
	HTS	m.14390C>Y	Yes	MT-ND6	novel, predicted damaging
	HTR	m.15598C>Y	Yes	MT-CYB	novel, synonymous
	No Therapy	m.3287C>A	Yes	MT-TL1	associated with encephalomyopathy
	No Therapy	m.9808C>T	Yes	MT-CO3	novel, predicted damaging
	No Therapy	m.14390C>Y	Yes	MT-ND6	novel, predicted damaging
	HS27	m.1102A>G	Yes	MT-RNR1	novel
	HMF	none			

	Cell Line	mtDNA position	Present in EVs	Gene
Significance: Polymorphisms	HS27	m.3550G>R	Yes	MT-ND1
	HS27	m.3741C>T	Yes	MT-ND1
	HS27	m.5529A>G	Yes	MT-TW
	HS27	m.8684C>T	Yes	MT-ATP6
	HS27	m.571C>A	Yes	D-LOOP
	HMF	m.9150A>G	Yes	MT-ATP6
	HMF	m.9380G>A	Yes	MT-CO3

Table S2.Cell line specific mitochondrial DNA variants (mutations and polymorphisms) and their presence in the extracellular vesicles (EVs).

Table S3. Mass Spectrometry analysis of mCAF derived EVs.

Accession	Description	Protein Abundancy (Area)	Molecular Function
P63260P68033 P62737 E9Q5F4	Actin, cytoplasmic 2,1, aortic smooth muscle, alpha cardiac muscle	1.523E10	protein bindin
E9PVA8	Protein Gcn1l1	1.100E10	protein binding; RNA bindin
Q5SX22	Polyubiquitin-B (Fragment) OS=Mus musculus GN=Ubb PE=2 SV=2 - [Q5SX22_MOUSE]	9.567E9	protein bindin
Q8BFZ3	Beta-actin-like protein 2	8.967E9	nucleotide bindin
P11438 P17047	Lysosome-associated membrane glycoprotein 2,1	5.754E9	protein bindin
P16045 P16110	Galectin-1,3	4.964E9	protein binding; signal transducer activity; RNA bindin
P41731	CD63 antigen	4.939E9	protein bindin
P70696 P10854 Q8CGP0	Histone H2B type 1-A, type 1-M, type 3-B	4.379E9	DNA binding; protein bindin
F8WIX8 Q8CGP6 Q64522 P0C0S6	Histone H2A, type 1-H, 2-B, Z,	3.867E9	DNA binding; protein bindin
P63017	Heat shock cognate 71 kDa protein	3.248E9	nucleotide binding; protein binding; RNA binding; catalyti activit
Q3TMX0	MCG4375, isoform CRA_b	3.105E9	protein bindin
Q9CQV8-2	Isoform Short of 14-3-3 protein beta/alpha	3.003E9	
P63101 P62259 P68510 P61982 P68254	14-3-3 protein zeta/delta, gamma, theta, eta, epsilon	2.991E9	protein,RNA,and DNA bindin
P17182	Alpha-enolase	2.949E9	RNA binding; protein binding; metal ion bindin
P08207 P50543 P97352 P07091 P14069	Protein S100-A10, A11, A13, A4, A6	2.933E9	metal ion binding; protein bindin
E9PZ00	Sulfated glycoprotein 1	2.887E9	protein bindin
P01831	Thy-1 membrane glycoprotein	2.705E9	enzyme regulator activity; protein bindin
P01942	Hemoglobin subunit alpha	2.622E9	antioxidant activity; catalytic activity; transporter activity metal ion binding; protein bindin
P21956-2	Isoform 2 of Lactadherin	2.540E9	protein bindin
P16858	Glyceraldehyde-3-phosphate dehydrogenase	2.517E9	catalytic activity; protein binding; nucleotide bindin
Q62351	Transferrin receptor protein 1	2.380E9	protein binding; RNA binding; receptor activity; transporte activity; catalytic activit
P17156	Heat shock-related 70 kDa protein 2	2.222E9	nucleotide binding; protein bindin
P35762	CD81 antigen OS	2.114E9	protein bindin
P40240	CD9 antigen	2.047E9	protein bindin
P52480-2	Isoform M1 of Pyruvate kinase isozymes M1/M2	1.898E9	nucleotide binding; metal ion binding; catalytic activity protein binding; RNA bindin
P52480	Pyruvate kinase isozymes M1/M2	1.898E9	nucleotide binding; metal ion binding; catalytic activity protein binding; RNA bindin
P18760 P45591	Cofilin-1 and2	1.800E9	protein bindin
F6TFF2	Pituitary tumor-transforming gene 1 protein-interacting protein (Fragment)	1.786E9	receptor activit
P84228 P02301	Histone H3.2 and 3C	1.727E9	DNA binding; protein bindin
P23242	Gap junction alpha-1 protein	1.726E9	signal transducer activity; protein binding; transporte activit
P62204	Calmodulin	1.649E9	metal ion binding; protein binding; enzyme regulato activit
P26041	Moesin	1.508E9	RNA binding; protein bindin
P05064 A6ZI47 Q9CPQ9	Fructose-bisphosphate aldolase A, aldolase, aldolase	1.501E9	protein binding; catalytic activity; RNA bindin
Q9D8N0 P10126 P62631 O70251	Elongation factor 1-gamma, beta, alpha 1 and 2	1.486E9	RNA binding; protein bindin
P11370	Retrovirus-related Env polyprotein from Fv-4 locus]	1.480E9	structural molecule activit
P97384, P07356, O35639, P97429, P48036 P14824,Q07076, F8WIT2 P10107	Annexin, A11, A7, A3, A6, A, A4, A1, A5, A2	1.478E9	RNA binding; protein binding; metal ion bindin
Q9WU78	Programmed cell death 6-interacting protein	1.467E9	protein bindin
P17742	Peptidyl-prolyl cis-trans isomerase A	1.425E9	catalytic activity; protein binding; RNA bindin
Q07797	Galectin-3-binding protein	1.353E9	receptor activity; protein bindin
Q91XV3	Brain acid soluble protein 1	1.343E9	protein binding; DNA bindin
F6SJ35	Protein Gm5068	1.275E9	
Q61696	Heat shock 70 kDa protein 1A	1.262E9	nucleotide binding; protein binding; RNA binding; catalyti activit

Q9D6P8	Calmodulin-like protein 3	1.260E9	metal ion bindin
P08752	Guanine nucleotide-binding protein G(i) subunit alpha-2	1.174E9	nucleotide binding; protein binding; catalytic activity; signa transducer activity; metal ion bindin
Q64253	Lymphocyte antigen 6E	1.161E9	
Q9DC51	Guanine nucleotide-binding protein G(k) subunit alpha	1.145E9	nucleotide binding; protein binding; catalytic activity; signa transducer activity; metal ion bindin
P18872-2	Isoform Alpha-2 of Guanine nucleotide-binding protein G(o) subunit alpha	1.145E9	nucleotide binding; catalytic activity; signal transduce activity; protein binding; metal ion bindin
Q99J93 Q9CQW9	Interferon-induced transmembrane protein 2 and 3	1.126E9	
P20029	78 kDa glucose-regulated protein	1.109E9	nucleotide and protein binding; enzyme regulator activit
P07901 P11499	Heat shock protein HSP 90-alpha and beta	1.055E9	nucleotide binding; RNA binding; protein binding; catalyti activity; enzyme regulator activit
P62874 P62880 Q61011	Guanine nucleotide-binding protein G(I)/G(S)/G(T) subunit beta-1,2,3	1.033E9	protein binding; catalytic activity; signal transducer activit
P20065-2	Isoform Short of Thymosin beta-4	1.032E9	protein bindin
Q9Z0J0	Epididymal secretory protein E1	1.016E9	protein bindin
P26645	Myristoylated alanine-rich C-kinase substrate	9.985E8	protein bindin
Q9CWJ9	Bifunctional purine biosynthesis protein PURH	9.978E8	catalytic activity; protein bindin
Q3TLP8	RAS-related C3 botulinum substrate 1, isoform CRA_a	9.626E8	nucleotide binding; catalytic activity; protein bindin
P06151	L-lactate dehydrogenase A chain	9.536E8	nucleotide binding; catalytic activity; protein bindin
Q9DCK3 H3BL26	Tetraspanin-4, 6 (fragment)	9.397E8	protein bindin
P09411 P09041	Phosphoglycerate kinase 1,2	8.908E8	nucleotide binding; catalytic activit
	Histone H4	8.877E8	DNA binding; protein binding; RNA bindin
K3W4Q8	Basigin	8.733E8	protein bindin
Q9DBJ1	Phosphoglycerate mutase 1	8.723E8	catalytic activity; protein bindin
P63094	Guanine nucleotide-binding protein G(s) subunit alpha isoforms short	8.676E8	nucleotide binding; protein binding; catalytic activity; signa transducer activity; metal ion bindin
P60766	Cell division control protein 42 homolog	8.663E8	nucleotide binding; catalytic activity; protein bindin
P34884	Macrophage migration inhibitory factor	8.443E8	catalytic activity; protein bindin
Q8BFR4	N-acetylglucosamine-6-sulfatase	8.150E8	catalytic activity; metal ion bindin
P26040	Ezrin	8.140E8	protein binding; RNA bindin
P26043	Radixin	8.140E8	protein binding; RNA bindin
P21550	Beta-enolase	8.111E8	metal ion and protein binding; catalytic activit
Q62465	Synaptic vesicle membrane protein VAT-1 homolog	7.999E8	nucleotide binding; metal ion binding; catalytic activit
P10852	4F2 cell-surface antigen heavy chain	7.986E8	RNA and protein bindin
P62835 Q99JI6 Q80ZJ1 P61226 Q8BU31	Ras-related protein Rap-1A, 1b, 2a, 2b,2c	7.902E8	nucleotide binding; catalytic activity; protein binding transporter activit
Q6GT24 P35700 Q61171 O08807	Peroxiredoxin 6,1, 2, 4	7.732E8	catalytic activity; antioxidant activity; protein bindin
Q9D379	Epoxide hydrolase 1	7.597E8	catalytic activity; protein bindin
A1L317 Q6IFX2	Keratin, type I cytoskeletal 24 and 42	7.269E8	structural molecule activit
Q9QUI0	Transforming protein RhoA	7.052E8	nucleotide binding; catalytic activity; protein bindin
Q9WV91	Prostaglandin F2 receptor negative regulator	6.769E8	protein bindin
E9Q616	Protein Ahnak	6.753E8	protein binding; RNA binding; structural molecule activit
P62962	Profilin-1	6.702E8	enzyme regulator activity; nucleotide binding; protei binding; RNA bindin
Q64337-2	Isoform 2 of Sequestosome-1	6.642E8	protein binding; metal ion bindin
Q64337	Sequestosome-1	6.642E8	protein binding; metal ion bindin
Q9JJ00 Q9JIZ9	Phospholipid scramblase 3,1	6.342E8	protein binding; transporter activit
P10605 P18242 Q9WUU7	Cathepsin B, D, Z	6.340E8	catalytic activity; protein bindin
Q9R0P5	Destrin	6.082E8	protein bindin
P58252	Elongation factor 2	5.947E8	nucleotide binding; RNA binding; catalytic activity; protei binding; translation regulator activit

Q9R0P3	S-formylglutathione hydrolase	5.945E8	catalytic activit
Q60932-2	Isoform Mt-VDAC1 of Voltage-dependent anion-selective channel protein 1	5.905E8	nucleotide binding; transporter activity; protein bindin
P53986 P57787	Monocarboxylate transporter 1,4	5.735E8	transporter activity; protein bindin
P10649 P15626 E9PV63	Glutathione S-transferase Mu 1, Mu 2, Mu 5	5.580E8	catalytic activity; protein binding; metal ion bindin
P17751	Triosephosphate isomerase	5.464E8	catalytic activity; protein bindin
Q8VDN2 Q6PIC6 Q9WV27 P97370	Sodium/potassium-transporting ATPase subunit alpha-1, alpha-3, alpha-4, beta-3	5.344E8	nucleotide binding; catalytic activity; transporter activity protein binding; metal ion bindin
E9PYB0 F7CVJ5 F7DBB3	Protein Ahnak2 (Fragment) (x3)	5.330E8	protein bindin
P15532 E9PZF0	Nucleoside diphosphate kinase, A	5.243E8	nucleotide binding; catalytic activit
P17183	Gamma-enolase	5.055E8	metal ion binding; catalytic activity; protein bindin
P62746 Q62159 P84096 Q8R527	Rho-related GTP-binding protein RhoB,Q,C,J,G	5.054E8	nucleotide binding; protein bindin
Q8R366	Immunoglobulin superfamily member 8	5.001E8	protein bindin
A2A839 P54116	Erythrocyte protein band 4.1 and 7 integral membrane	4.883E8	protein binding; structural molecule activit
P21278 P27601 P30677 P68040 P29387	Guanine nucleotide-binding protein subunit beta-2-like 1,beta-1,beta-4, alpha-13,alpha-11,alpha-14	4.829E8	RNA bindin
Q9WVK4Q8BH64 Q9QXY6	EH domain-containing protein 1,2,3	4.803E8	nucleotide binding; catalytic activity; metal ion binding protein bindin
G3UX26	Voltage-dependent anion-selective channel protein 2 (Fragment)	4.803E8	transporter activit
P15379-2	Isoform 13 of CD44 antigen	4.764E8	catalytic activity; receptor activity; signal transduce activity; protein bindin
Q8R2Q8	Bone marrow stromal antigen 2	4.750E8	RNA and protein bindin
P61027 P62492 P46638 Q9DD03 Q91V41 P35293 P62821 Q9D1G1 P35282 P35285 P53994 Q921E2 Q6PHN9 D3YWL1 Q8CG50 P56371 Q91ZR1 Q9CQD1 P61021 P35278 P35279 P51150 P55258 P61028 Q9R0M6	Ras-related protein Rab-22A, 43, 1A, 8A, 8B, 1B, 10, 35, 4A, 3D (FRAG), 4B, 13,21,18,11A,11B,14,5C,5B,5A,6A,9A,2A,31,7A	4.665E8	nucleotide binding; catalytic activity; protein bindin
Q99PT1	Rho GDP-dissociation inhibitor 1	4.634E8	enzyme regulator activity; protein bindin
P04104 Q6IFZ6 Q3UV17 Q8VED5	Keratin, type II cytoskeletal 1, 1b, 2 oral, 79	4.588E8	structural molecule activit
G3XA41	MCG50219	4.517E8	
P11276	Fibronectin	4.490E8	protein binding; enzyme regulator activity; metal io bindin
Q9DAS9	Guanine nucleotide-binding protein G(I)/G(S)/G(O) subunit gamma-12	4.410E8	signal transducer activity; protein bindin
P16675 O35114	Lysosomal protective protein and membrane protein 2	4.408E8	catalytic activity; protein bindin
Q9CYL5	Golgi-associated plant pathogenesis-related protein 1	4.264E8	protein bindin
Q9ER71-2	Isoform 2 of Rho-related GTP-binding protein RhoJ	4.255E8	nucleotide binding; catalytic activity; protein bindin
Q9ERD7 P68372 P99024 Q922F4	Tubulin beta-3, 4B, 5, 6 chains	4.216E8	nucleotide binding; catalytic activity; structural molecul activity; protein bindin
Q8VEH3, Q9CQW2	ADP-ribosylation factor-like protein 8A and 8B	4.212E8	nucleotide bindin
Q9CZR2	N-acetylated-alpha-linked acidic dipeptidase 2 USE]	4.190E8	catalytic activity; metal ion bindin
P13020-2	Isoform 2 of Gelsolin	4.176E8	protein binding; metal ion bindin
P08113	Endoplasmin	4.126E8	nucleotide binding; RNA binding; protein bindin
O09131 P19157	Glutathione S-transferase omega-1, P1	4.094E8	catalytic activity; protein binding; antioxidant activit
J3QPE8	MCG16555	4.090E8	transporter activit
Q9CX00	IST1 homolog	4.080E8	protein bindin
P09528	Ferritin heavy chain	3.858E8	catalytic activity; metal ion bindin
P15864P43277 P43274	Histone H1.4,3,2	3.766E8	DNA binding; protein binding; RNA bindin
Q9EQK5 E9Q3X0	Major vault protein (x2)	3.691E8	protein bindin
P50396 Q61598	Rab GDP dissociation inhibitor alpha, beta	3.678E8	enzyme regulator activity; protein bindin
Q61753	D-3-phosphoglycerate dehydrogenase	3.639E8	nucleotide binding; catalytic activit

Q60605	Myosin light polypeptide 6	3.620E8	catalytic activity; motor activity; metal ion binding; protei binding; structural molecule activit
P24638	Lysosomal acid phosphatase	3.582E8	protein binding; catalytic activit
Q6IRU2 P68373	Tropomyosin alpha-4, IC chains	3.548E8	protein binding; metal ion bindin
Q60854	Serpin B6	3.540E8	protein binding; enzyme regulator activit
O70404	Vesicle-associated membrane protein 8	3.523E8	protein bindin
Q9Z1Q5 Q9QYB1 Q8BXK9	Chloride intracellular channel protein 1,4,5	3.455E8	transporter activity; protein bindin
O88342	WD repeat-containing protein 1	3.426E8	protein bindin
O08917	Flotillin-1	3.422E8	protein bindin
Q6ZQ38	Cullin-associated NEDD8-dissociated protein 1	3.406E8	protein bindin
P70296	Phosphatidylethanolamine-binding protein 1	3.399E8	nucleotide binding; enzyme regulator activity; protei binding; RNA bindin
Q60648	Ganglioside GM2 activator	3.351E8	catalytic activity; transporter activity; enzyme regulato activit
P20152	Vimentin	3.324E8	protein binding; RNA binding; structural molecule activit
P10639	Thioredoxin	3.307E8	protein binding; catalytic activity; RNA bindin
A1BN54P57780	Alpha actinin 1a and 4	3.292E8	RNA binding; protein binding; metal ion bindin
O35604	Niemann-Pick C1 protein	3.275E8	transporter activity; protein binding; receptor activity; signa transducer activit
P40124	Adenylyl cyclase-associated protein 1	3.273E8	protein bindin
A2AKI5 P11688 P09055	Integrin alpha V, alpha 5, beta-1	3.211E8	protein binding; transporter activity; metal ion bindin
P40237	CD82 antigen	3.140E8	
F6VRP8	Galectin-3-binding protein (Fragment)	3.094E8	receptor activity; protein bindin
P06745	Glucose-6-phosphate isomerase	3.058E8	catalytic activity; protein bindin
P62965	Cellular retinoic acid-binding protein 1	3.057E8	transporter activit
G3UZ34	116 kDa U5 small nuclear ribonucleoprotein component	3.051E8	nucleotide binding; catalytic activit
Q62426	Cystatin-B	3.042E8	protein binding; enzyme regulator activity; RNA bindin
P68368	Tubulin alpha-4A chain	3.008E8	
Q9CPX4	Ferritin	2.978E8	metal ion binding; protein bindin
P14211	Calreticulin	2.909E8	protein binding; RNA binding; metal ion bindin
O54962	Barrier-to-autointegration factor	2.891E8	DNA bindin
Q91VR7	Microtubule-associated proteins 1A/1B light chain 3A	2.877E8	protein bindin
P45376	Aldose reductase	2.853E8	catalytic activit
Q9Z127	Large neutral amino acids transporter small subunit 1	2.850E8	transporter activit
O35566	CD151 antigen	2.848E8	protein bindin
Q68FD5	Clathrin heavy chain 1	2.791E8	RNA binding; structural molecule activity; protein bindin
F6SAC3	Glucose-6-phosphate isomerase	2.778E8	catalytic activit
Q61187	Tumor susceptibility gene 101 protein	2.722E8	protein bindin
P84084, P84078 Q8BSL7 P61750	ADP-ribosylation factor 5,4,2,1	2.674E8	nucleotide and protein binding; signal transducer activit
Q9ET22	Dipeptidyl peptidase 2	2.637E8	catalytic activit
J3QP68	Uncharacterized protein	2.623E8	
P63028	Translationally-controlled tumor protein	2.591E8	metal ion binding; protein binding; RNA bindin
Q05816	Fatty acid-binding protein, epidermal	2.583E8	transporter activit
Q3UW53	Protein Niban	2.579E8	
O70318	Band 4.1-like protein 2	2.560E8	protein binding; structural molecule activit
P50516	V-type proton ATPase catalytic subunit A	2.551E8	nucleotide binding; catalytic activity; transporter activit
Q920A5	Retinoid-inducible serine carboxypeptidase	2.538E8	catalytic activit
P63242	Eukaryotic translation initiation factor 5A-1	2.513E8	RNA binding; protein bindin

Q9WV92-3	Isoform 3 of Band 4.1-like protein 3	2.484E8	protein binding; structural molecule activit
Q9WV92-7	Isoform 7 of Band 4.1-like protein 3	2.484E8	protein binding; structural molecule activit
Q9WV92-8	Isoform 8 of Band 4.1-like protein 3	2.484E8	protein binding; structural molecule activit
P99029	Peroxiredoxin-5, mitochondrial	2.435E8	DNA binding; antioxidant activity; catalytic activity; protei binding; enzyme regulator activit
A2AUE1	DnaJ (Hsp40) homolog, subfamily C, member 5 (Fragment)	2.435E8	protein bindin
P46467 Q8VEJ9 Q9EQH3 D3Z645 Q9D1C8	Vacuolar protein sorting-associated protein 4A, 4B, 28 (homolog), 29, 35	2.430E8	nucleotide binding; catalytic activity; RNA binding; protei bindin
O89051	Integral membrane protein 2B	2.411E8	protein binding; nucleotide bindin
Q921W0 Q99LU0Q9CQD4 Q9DB34 Q9D8B3 Q9D7S9	Charged multivesicular body protein 1a, 4b, 1b-1,5,1b02,2a	2.399E8	protein bindin
Q9DCD6 Q8R3R8 P60521	Gamma-aminobutyric acid receptor-associated protein, like 1 and 2	2.393E8	protein bindin
P10833 P62071	Ras-related protein R-Ras, 2	2.378E8	nucleotide binding; catalytic activity; protein bindin
Q9WTI7-2	Isoform 2 of Unconventional myosin-Ic	2.354E8	catalytic activity; motor activity; nucleotide binding; protei bindin
Q80X71 F8WHW3	Transmembrane protein 106B,55B	2.341E8	catalytic activit
P29416, P20060	Beta-hexosaminidase subunit alpha and beta	2.336E8	catalytic activity; protein bindin
P21279	Guanine nucleotide-binding protein G(q) subunit alpha	2.325E8	nucleotide binding; protein binding; catalytic activity; signa transducer activity; enzyme regulator activity; metal io bindin
P21995	Embigin	2.321E8	protein bindin
Q9R0Q7	Prostaglandin E synthase 3	2.315E8	protein binding; catalytic activit
P39688 E9QPE2 Q04736	Tyrosine-protein kinase Yes, receptor , and Fyn	2.300E8	nucleotide binding; catalytic activity; protein bindin
P63321Q9JIW9	Ras-related protein Ral-A , B	2.288E8	nucleotide binding; catalytic activity; protein bindin
Q61735	Leukocyte surface antigen CD47	2.288E8	protein binding; receptor activity; signal transducer activit
P47757-2	Isoform 2 of F-actin-capping protein subunit beta	2.272E8	protein bindin
P49817	Caveolin-1	2.271E8	structural molecule and catalyic activitt
P49817-2	Isoform Beta of Caveolin-1	2.271E8	protein binding; catalytic activity; structural molecul activity; enzyme regulator activit
F8WJK8	Hsc70-interacting protein	2.270E8	protein bindin
Q9WV54	Acid ceramidase	2.239E8	catalytic activit
Q9ESU7	Neutral amino acid transporter ASCT2	2.230E8	transporter activit
Q61792	LIM and SH3 domain protein 1	2.228E8	protein binding; metal ion binding; transporter activit
P31786	Acyl-CoA-binding protein	2.192E8	protein bindin
O88947	Coagulation factor X	2.170E8	catalytic activity; metal ion binding; protein bindin
P08556	GTPase NRas	2.136E8	nucleotide binding; catalytic activity; transporter activity protein bindin
P16460	Argininosuccinate synthase	2.127E8	RNA binding; protein binding; metal ion bindin
Q9WV32, P61161, Q9CVB6, Q9JM76	Actin-related protein 2/3 complex subunit 1B, 2, 3	2.123E8	structural molecule activit
P01899 P01902	H-2 class I histocompatibility antigen, D-B alpha chain, K-D alpha chain	2.120E8	protein binding; RNA bindin
Q3TCN2	Putative phospholipase B-like 2	2.100E8	catalytic activit
Q9QZC7	Pleckstrin homology domain-containing family B member 2	2.090E8	protein bindin
P11983 P80314 P80315 P80313 P42932	T-complex protein 1 subunit delta, beta, theta, eta, alpha	2.087E8	nucleotide binding; protein binding; RNA bindin
Q61990-2	Isoform 2 of Poly(rC)-binding protein 2	2.077E8	DNA binding; RNA binding; protein bindin
Q9QWR8	Alpha-N-acetylgalactosaminidase	2.069E8	catalytic activity; protein bindin
P62774	Myotrophin	2.056E8	protein binding; DNA bindin
P40142	Transketolase	2.052E8	metal ion binding; catalytic activity; protein bindin
P27773 P09103	Protein disulfide-isomerase, A3	2.049E8	catalytic activity; metal ion binding; protein binding; RN bindin
P58774-2	Isoform 2 of Tropomyosin beta chain	2.034E8	protein binding; structural molecule activit
P50428, P50429	Arylsulfatase A and B	2.017E8	catalytic activity; metal ion bindin
Q01853	Transitional endoplasmic reticulum ATPase	2.012E8	nucleotide binding; catalytic activity; RNA binding; protei

			binding; enzyme regulator activit
Q8C129	Leucyl-cystinyl aminopeptidase	2.008E8	receptor activity; signal transducer activity; catalyti activity; protein binding; metal ion bindin
O89023	Tripeptidyl-peptidase 1	2.008E8	catalytic activity; protein binding; metal ion bindin
Q9D1A2	Cytosolic non-specific dipeptidase	2.006E8	catalytic activity; metal ion bindin
Q8BH40 Q9ER005	Syntaxin 7, 12	1.992E8	protein bindin
P60335	Poly(rC)-binding protein 1	1.974E8	DNA binding; RNA binding; protein binding; translatio regulator activit
Q9CQ22 O88653 Q9D1L9	Ragulator complex protein LAMTOR1,3,5	1.969E8	protein binding; structural molecule activit
P51655	Glypican-4	1.965E8	protein bindin
P63037 Q9QYJ0	DnaJ homolog subfamily A member 1, 2	1.955E8	protein binding; nucleotide binding; metal ion bindin
P32883-2	Isoform 2B of GTPase KRas	1.923E8	nucleotide binding; catalytic activity; protein binding transporter activit
E9Q9C5	V-type proton ATPase 16 kDa proteolipid subunit (Fragment)	1.914E8	protein binding; catalytic activity; transporter activit
P20352	Tissue factor	1.905E8	protein binding; receptor activity; signal transducer activit
O88952	Protein lin-7 homolog C	1.900E8	protein bindin
G5E829	MCG13663, isoform CRA_a	1.896E8	nucleotide binding; catalytic activity; transporter activity protein binding; metal ion bindin
Q9WVJ3-2	Isoform 2 of Carboxypeptidase Q	1.871E8	catalytic activit
Q9R118	Serine protease HTRA1	1.849E8	catalytic activity; protein bindin
Q9DCD0	6-phosphogluconate dehydrogenase, decarboxylating	1.823E8	nucleotide binding; catalytic activit
Q8BP47	Asparagine--tRNA ligase, cytoplasmic	1.823E8	nucleotide binding; catalytic activit
Q78ZA7	Nucleosome assembly protein 1-like 4	1.813E8	RNA bindin
Q00780	Collagen alpha-1(VIII) chain	1.799E8	protein bindin
Q8BGQ7	Alanine--tRNA ligase, cytoplasmic	1.798E8	RNA, nucleotide,protein and metal ion bindin
Q9DCN2-2	Isoform 2 of NADH-cytochrome b5 reductase 3	1.793E8	catalytic activity; protein binding; nucleotide bindin
Q9JII6	Alcohol dehydrogenase [NADP(+)]	1.755E8	catalytic activit
Q64727	Vinculin	1.751E8	protein binding; catalytic activity; structural molecul activit
D3Z2H9	Uncharacterized protein	1.737E8	
P47754	F-actin-capping protein subunit alpha-2	1.733E8	protein bindin
Q69ZN7 E9Q390	Myoferlin (x2)	1.725E8	protein bindin
Q6P9J9	Anoctamin-6	1.711E8	transporter activity; protein bindin
Q8K2Q7	BRO1 domain-containing protein BROX	1.689E8	
P62827	GTP-binding nuclear protein Ran	1.681E8	nucleotide binding; catalytic activity; protein binding; RN bindin
G5E8R0	Tropomyosin 1, alpha, isoform CRA_i	1.669E8	protein binding; structural molecule activit
Q8K0Z5	Tropomyosin 3, gamma	1.669E8	protein bindin
P08228	Superoxide dismutase [Cu-Zn]	1.647E8	antioxidant activity; catalytic activity; metal ion binding protein bindin
P17809	Solute carrier family 2, facilitated glucose transporter member 1	1.589E8	transporter activity; protein bindin
Q9R0Y5	Adenylate kinase isoenzyme 1	1.589E8	nucleotide binding; catalytic activit
Q6P069-2	Isoform 2 of Sorcin]	1.582E8	protein binding; catalytic activity; metal ion bindin
Q8VEM8	Phosphate carrier protein, mitochondrial	1.554E8	transporter activity; protein bindin
Q99JY9	Actin-related protein 3	1.547E8	nucleotide and protein bindin
Q8VDD5	Myosin-9	1.546E8	catalytic activity; motor activity; nucleotide binding; protei binding; RNA bindin
Q9WVA4	Transgelin-2	1.531E8	protein bindin
Q91YR1	Twinfilin-1	1.524E8	protein binding; catalytic activity; nucleotide bindin
Q8VHX6-2	Isoform 2 of Filamin-C	1.518E8	protein bindin
Q6ZWQ5 Q78ZM0	Sorting nexin 12,3	1.497E8	protein bindin

B7FAU9	Filamin, alpha	1.494E8	protein binding; signal transducer activity; RNA bindin
Q8CI59	Metalloreductase STEAP3	1.475E8	nucleotide binding; catalytic activity; metal ion bindin
P70349	Histidine triad nucleotide-binding protein 1	1.431E8	nucleotide binding; catalytic activit
Q3UKC1	Tax1-binding protein 1 homolog	1.423E8	catalytic activity; motor activity; protein binding; metal io bindin
P57776-2	Isoform 2 of Elongation factor 1-delta	1.410E8	RNA bindin
P50518 P51863 P62814	V-type proton ATPase subunit E 1, D1, B1 brain isoform	1.393E8	protein binding; catalytic activity; transporter activit
Q8BH78	RTN4	1.383E8	protein binding; RNA bindin
P70168	Importin subunit beta-1	1.381E8	protein binding; transporter activity; RNA bindin
O35598	Disintegrin and metalloproteinase domain-containing protein 10	1.380E8	catalytic activity; protein binding; metal ion bindin
Q9JKF1	Ras GTPase-activating-like protein IQGAP1	1.375E8	enzyme regulator activity; protein bindin
P12815	Programmed cell death protein 6	1.362E8	catalytic activity; metal ion binding; protein bindin
Q6ZWZ6, P25444 P62242	40S ribosomal protein S12, S8, S2	1.350E8	RNA bindin
Q91XX1	Protein Pcdhga11	1.337E8	metal ion bindin
Q3TYX2	LRRN4 C-terminal-like protein	1.328E8	protein bindin
O88668	Protein CREG1	1.327E8	protein binding; nucleotide binding; catalytic activit
Q99K51	Plastin-3	1.311E8	protein binding; metal ion bindin
Q32ME1	ATPase, Ca++ transporting, plasma membrane 4	1.305E8	nucleotide, protei, metal ion bindin
P51569	Alpha-galactosidase A	1.300E8	catalytic activity; protein bindin
Q6X893	Choline transporter-like protein 1	1.285E8	transporter activit
D3Z6C3	Uncharacterized protein	1.271E8	structural molecule activit
P26231	Catenin alpha-1	1.266E8	structural molecule activity; protein binding; RNA bindin
H3BKL7	Deoxyribonuclease-1	1.251E8	catalytic activit
Q99LX0	Protein DJ-1	1.239E8	RNA binding; antioxidant activity; catalytic activity; protei binding; metal ion binding; enzyme regulator activit
O70589-3	Isoform 3 of Peripheral plasma membrane protein CASK	1.236E8	nucleotide binding; catalytic activity; protein bindin
D3Z5U5	P2X purinoceptor (Fragment)	1.227E8	receptor activity; signal transducer activity; transporte activity; nucleotide bindin
Q9WVE8	Protein kinase C and casein kinase substrate in neurons protein 2	1.225E8	protein binding; catalytic activit
Q9DB05	Alpha-soluble NSF attachment protein	1.222E8	protein bindin
P46935	E3 ubiquitin-protein ligase NEDD4	1.222E8	catalytic activity; protein bindin
P34022	Ran-specific GTPase-activating protein	1.217E8	enzyme regulator activit
Q61553	Fascin	1.214E8	protein binding; RNA bindin
E9QAZ2	Ribosomal protein L15	1.205E8	structural molecule activit
Q9CZD3	Glycine--tRNA ligase	1.201E8	nucleotide binding; catalytic activity; protein bindin
Q8CCK0	Core histone macro-H2A.2	1.194E8	DNA binding; protein bindin
O08553	Dihydropyrimidinase-related protein 2	1.176E8	protein binding; catalytic activit
Q8C7B4	Gamma-glutamyltransferase 5	1.166E8	catalytic activit
Q91ZX7	Prolow-density lipoprotein receptor-related protein 1	1.166E8	protein binding; metal ion binding; RNA bindin
P70699	Lysosomal alpha-glucosidase	1.158E8	catalytic activit
P61971	Nuclear transport factor 2	1.157E8	protein binding; transporter activit
Q9Z2U1	Proteasome subunit alpha type-5	1.149E8	catalytic activit
Q60634-3	Isoform 3 of Flotillin-2	1.140E8	protein bindin
Q91XH6	Vesicle transport through interaction with t-SNAREs 1B homolog	1.133E8	protein bindin
Q60598	Src substrate cortactin	1.123E8	protein bindin
E9PUX4P14115 P27659 Q6ZWV7	60S ribosomal protein L6, L3, L35, L27A	1.118E8	structural molecule activit
Q00612	Glucose-6-phosphate 1-dehydrogenase X	1.115E8	nucleotide binding; catalytic activity; protein bindin

O08997	Copper transport protein ATOX1	1.115E8	transporter activity; metal ion binding; protein bindin
O70475	UDP-glucose 6-dehydrogenase	1.108E8	nucleotide binding; catalytic activit
P51881,P48962	ADP/ATP translocase 1, 2	1.085E8	transporter activit
P99027	60S acidic ribosomal protein P2	1.079E8	structural molecule activit
O88844	Isocitrate dehydrogenase [NADP] cytoplasmic	1.077E8	metal ion binding; catalytic activity; protein bindin nucleotide bindin
E9QNH6	Unconventional myosin-Ib	1.073E8	catalytic activity; motor activity; nucleotide binding; protei bindin
P26618	Platelet-derived growth factor receptor alpha	1.072E8	nucleotide binding; catalytic activity; receptor activity signal transducer activity; protein bindin
Q61768	Kinesin-1 heavy chain	1.072E8	nucleotide binding; catalytic activity; motor activity; protei binding; transporter activit
P45377	Aldose reductase-related protein 2	1.068E8	catalytic activit
P83940	Transcription elongation factor B polypeptide 1	1.062E8	catalytic activity; protein bindin
Q9D0R2	Threonine--tRNA ligase, cytoplasmic	1.054E8	nucleotide binding; catalytic activit
P62137 P63087	Serine/threonine-protein phosphatase PP1-gamma and alpha catalytic subunit	1.052E8	catalytic activity; protein binding; RNA binding; metal io bindin
P14152	Malate dehydrogenase, cytoplasmic	1.048E8	nucleotide binding; catalytic activit
P37889-2	Isoform 2 of Fibulin-2	1.041E8	metal ion binding; protein bindin
Q60864	Stress-induced-phosphoprotein 1	1.031E8	protein binding; RNA bindin
Q99LD8	N(G),N(G)-dimethylarginine dimethylaminohydrolase 2	1.025E8	catalytic activit
P12265	Beta-glucuronidase	1.014E8	catalytic activity; protein bindin

Table S3. Mass Spectrometry analysis of mCAF derived EVs, mCAFs were isolated from HTR xenografts (Figure 2), cultured in vitro and EVs were isolated. Identified peptides were filtered using 1% False Discovery Rate (FDR) and Percolator (Kall et al, Nat Methods. 2007 Nov;4(11):923-5). Proteins were sorted out according to estimated abundance, which is represented in the column titled "Area". The area is calculated based on the most abundant peptides for the respective protein (Silva et al, Mol Cell Proteomics. 2006 Jan;5(1):144-56). Proteins not detected or present in low amounts are assigned an area zero. Proteins are annotated according to their molecular function, cellular component and biological process.Data were extracted and queried against Uniprot Mouse using Proteome Discoverer and Mascot. Potential common Fetal Bovine Serum and human contaminants were included in the Mouse database and were labeled "CON" in the column "Accession" (Bunkenborg et al, Proteomics. 2010, Aug;10(16):3040-4).

Table S4. Primers used in the study

Murine Mitochondrial Primers (Tan et al[2])

Murine Mitochondrial DNA					
Gene	**Sequence 5'-3'**	**Position**	**Length (bps)**	**Assay**	**Reference**
DLoop	AGGTTTGGTCCTGGCCTTAT	72 F	149	Real Time/PCR	SnapeGene Viewer Software
	GTGGCTAGGCAAGGTGTCTT	221 R			
ND1 (1)	CTAGAAACCCCGAACCAAA	1323 F	105		
	CCAGCTATCACCAAGCTCGT	1428 R			
ND1 (2)	CAGCCGGCCCATTCGCGTTA	3398 F	197		
	AGCGGAAGCGTGGATAGGATGC	3595 R			
ND2	TCCTCCTGGCCATCGTACTCAACT	4123 F	131		
	AGAAGTGGAATGGGGCGAGGC	4254 R			
COX1	CCAGTGCTAGCCGCAGGCAT	5927 F	127		
	TCTGGGTGCCCAAAGAATCAGAACA	6054 R			
COX2	AGTTGATAACCGAGTCGTTCTGCCA	7425 F	123		
	TCGGCCTGGGATGGCATCAGT	7548 R			
ATP8	ATGCCACAACTAGATACATCAACA	7768F	176		
	GGGGTAATGAATGAGGCAAA	7944R			
ATP6	GCTCTCACTCGCCCACTTCCTTCC	8297 F	529		
	GCCGGACTGCTAATGCCATTGGTT	8826 R			
COX3	ACCTACCAAGGCCACCACACTCC	8804 F	149		
	GCAGCCTCCTAGATCATGTGTTGGT	8953 R			
ND3	ACCCTACAAGCTCTGCACGCC	9585 F	385		
	GCTCATGGTAGTGAAGTAGAAGGGCA	9970 R			
ND4 L	TCGCTCCCACCTAATATCCACATTGC	9945 F	141		
	GCAGGCTGCGAAAACCAAGATGG	10086 R			
ND4	TCGCCTACTCCTCAGTTAGCCACA	11026 F	115		
	TGATGATGTGAGGCCATGTGCGA	11141 R			
ND5	TCGGAAGCCTCGCCCTCACA	12868 F	105		
	AGTAGGGCTCAGGCGTTGGTGT	12973 R			
ND6	AATACCCGCAAACAAAGATCACCCAG	13585 F	99		
	TGTTGGGGTTATGTTAGAGGGAGGGA	13684 R			
Cytb	ACAGCAAACGGAGCCTCAA	14394 F	134		
	TGCTGTGGCTATGACTGCGAACA	14528 R			

Human Mitochondrial Primers

Human Mitochondrial DNA-RNA					
Gene	**Sequence 5'-3'**	**Position**	**Length (bps)**	**Assay**	**Reference**
DLoop	TGGCCACAGCACTTAAACACATCTC	321 F	175	Real Time/PCR	SnapGene Viewer Software
	GGGTTGTATTGATGAGATTAGTAGTATGGGAG	496 R			
12S	CCCGTTCCAGTGAGTTCACCC	706 F	112		
	TGTGGGGGTGCCCTTTGTC	818 R			
16S	AACTTTGCAAGGAGAGCCAAAGC	1873 F	205		
	GGGATTTAGAGGGTTCTGTGGGC	2078 R			
ND1	ACGCCATAAAACTCTTCACCAAAG	3458 F	103	Real Time/PCR	
	TAGTAGAAGAGCGATGGTGAGAGCTA	3561 R			
ND2	CTTCTGAGTCCCAGAGGTTACCCA	4805 F	182	Real Time/PCR	
	CCGTCAACTCCACCTAATTTGGTTTG	4987 R			
COX1	TGCCATAACCCAATACCAAACGC	6425 F	112		
	CTGTTAGTAGTATAGTGATGCCAGCAGCTAGG	6537 R			
COX2	CTACGGTCAATGCTCTGAAATCTGTG	8161 F	153		
	GCTAAGTTAGCTTTACAGTGGGCTCTAG	8314 R			
ATP6	GAAAATCTGTTCGCTTCATTCATTGCC	8533 F	138		
	GCTGATTAGTGGTGGGTTGTTACTG	8671 R			
COX3	CGATACGGGATAATCCTATTTATTACCTCAG	9444 F	199		
	CAGGTGATTGATACTCCTGATGCGA	9643 R			
ND3	CATTTTGACTACCACAACTCAACGGCTAC	10120 F	160		
	GGGTAAAAGGAGGGCAATTTCTAGATC	10280 R			

ND4L	GCTACTCTCATAACCCTCAACACCC	10599 F	130		
	AGGCCATATGTGTTGGAGATTGAGA	10729 R			
ND4	CCAACGCCACTTATCCAGTG	10999 F	237		
	GGGAAGGGAGCCTACTAGGGTGT	11236 R			
ND5	TTACCACCCTCGTTAACCCTAACAAA	12395 F	165	Real Time/PCR	
	TGGGTTGTTTGGGTTGTGGCT	12560 R			
ND6	ACGCCCATAATCATACAAAGCCC	14224 F	149	Real Time/PCR	
	GGATTGGTGCTGTGGGTGAAA	14373 R			
Cyt-b	CGCCTGCCTGATCCTCCAA	14860 F	191		
	AGGCCTCGCCCGATGTGTAG	15051 R			
Mito 1	[aminoC6]ACATAGCACATTACAGTCAAATCCCTTCTCGTCCCC	16331 F	3968	Long PCR	Dames S., et al[1]
	[aminoC6]TGAGATTGTTTGGGCTACTGCTCGCAGTGC	3729 R			
Mito 2	[aminoC6]TACTCAATCCTCTGATCAGGGTGAGCATCAAACTC	3646 F	5513		
	[aminoC6]GCTTGGATTAAGGCGACAGCGATTTCTAGGATAGT	9458 R			
Mito 3	[aminoC6]TCATTTTTATTGCCACAACTAACCTCCTCGGACTC	8753 F	9289		
	[aminoC6]CGTGATGTCTTATTTAAGGGGAACGTGTGGGCTAT	16566 R			

Housekeeping Primers Human (nDNA)

Housekeeping Genes						
Gene	**Sequence**	**Position**	**Length (bps)**	**Assay**	**Target**	**Reference**
ACTB	AGGATCTTCATGAGGTAGTCAGTCAG	1358 F	98	Real Time	DNA	Clone Manager 9 (Sci-Ed Software)
	CCACACTGTGCCCATCTACG	1456 R				
GAPDH	CTCTGCTCCTCCTGTTCGAC	5030 F	126	Real Time/PCR	DNA	SnapGene Viewer Software
	CGCCCGCGTCCGGCCTACACA	5156 R				
ACTB	ACCAACTGGGACGACATGGAG	313 F	379	PCR	RNA	Clone Manager 9 (Sci-Ed Software)
	GTGGTGGTGAAGCTGTAGCC	692 R				

Housekeeping Primers Murine (nDNA)

Housekeeping Genes						
Gene	**Sequence**	**Position**	**Length (bps)**	**Assay**	**Target**	**Reference**
GAPDH	AGCAGCCGCATCTTCTTGTGCAGTG	38,619,737	226	Real Time/PCR	DNA/RNA	SnapGene Viewer Software
	GGCCTTGACTGTGCCGTTGAATTT	38,619,962				
COX4	ATTGGCAAGAGAGCCATTTCTAC	160	100	Real Time/PCR	DNA/RNA	Tan et al[2]
	CACGCCGATCAGCGTAAGT	259				

References

1. Dames, S., Eilbeck, K. & Mao, R. A high-throughput next-generation sequencing assay for the mitochondrial genome. *Methods in molecular biology* **1264**, 77-88 (2015).
2. Tan, A.S. *et al.* Mitochondrial genome acquisition restores respiratory function and tumorigenic potential of cancer cells without mitochondrial DNA. *Cell metabolism* **21**, 81-94 (2015).